Molybdenum−Iron Sulfide-Bridged Double Cubanes

Jiesheng Huang, Subhashish Mukerjee, Brent M. Segal, Haruo Akashi, Jian Zhou, and R. H. Holm*

Contribution from the Department of Chemistry and Chemical Biology, Harvard University, Cambridge, Massachusetts 02138

Received May 2, 1997[⊗]

Abstract: A new class of clusters, sulfide-bridged double cubanes containing the units $MFe_3(\mu_3\text{-}S)_4$ (M = Fe, Mo), has been investigated as possible synthetic precursors to the iron−molybdenum cofactor (FeMoco) of nitrogenase. Clusters containing the symmetric core structures $[Fe_4Q_4\text{-}Q\text{-}Fe_4Q_4]^{2+}$ (**11**−**13**, Q = S, Se) have been prepared by the coupling of separate cubane clusters ($[Fe_4S_4Cl_4]^{2-}$, $[Fe_4Q_4(LS_3)Cl]^{2-}$, where LS_3 = 1,3,5-tris((4,6-dimethyl-3-mercaptophenyl)thio)-2,4,6-tris(*p*-tolylthio)benzenate(3−)). Similarly, the cuboidal cluster $[VFe_4S_6(PEt_3)_4Cl]$ was coupled to form $[VFe_4S_6(PEt_3)_4]_2S$ (**14**). The cluster $[(Fe_4S_4Cl_3)_2S]^{4-}$ (**11**) is the first structurally proven example of the class (Challen, P. R.; Koo, S.-M.; Dunham, W. R.; Coucouvanis, D. *J. Am. Chem. Soc.* **1990**, *112*, 2455). Bridged structures have also been established crystallographically for $\{[Fe_4Se_4(LS_3)]_2Se\}^{4-}$ (**13**) and **14**. Other criteria for identification of this structure developed using **11**−**14** are coupled redox processes in cyclic voltammetry and the detection of intact double cubane ions by electrospray mass spectrometry. For the coupling of heterometal cubanes, the Mo site was protected by chelation with Meida (*N*-methylimidodiacetate(2−)) as in $[(Meida)MoFe_3S_4Cl_3]^{2-}$ (**6**), thereby directing the bridging reaction to the Fe sites. The structures of two $[VFe_3S_4]^{2+}$ cubane clusters containing the tricoordinate (Meida)V fragment are reported. The reaction system **6**/Li_2S afforded $\{[(Meida)MoFe_3S_4Cl_2]_2S\}^{4-}$ (**15**). The symmetrical sulfide-bridged double cubane structure of **15** has been established by the electrochemical and mass spectrometric criteria and by the existence of the four isomers consistent with this structure. The equimolar reaction system **6**/$[Fe_4S_4Cl_4]^{2-}$/Li_2S produced a mixture of $\{[(Meida)MoFe_3S_4Cl_2]S(Fe_4S_4Cl_3)\}^{4-}$ (**17**), **15**, and **11**. Cluster **17** is also formed in the system **15**/$[Fe_4S_4Cl_4]^{2-}$. The unsymmetrical sulfide-bridged double cubane structure of **17** was established by mass spectrometry and detection of the two isomers consistent with this structure. In the first reaction system, the product mole ratio **17**:**15** ≈ 3:1 is explained in terms of differential steric hindrance of conformations arising from rotation around the Fe−S−Fe bridge. The core composition of double cubane **15** ($Mo_2Fe_6S_9$) approaches that of FeMoco ($MoFe_7S_9$). The core composition of **17** is exactly the same as FeMoco; **17** is the first synthetic cluster with this property.

Introduction

We have described previously a group of native metal sites in proteins and enzymes as *bridged biological metal assemblies*, consisting of two discrete fragments juxtaposed wholly or in part by one or more covalent bridges.[1] Assemblies of this sort containing metal−sulfur clusters include *Escherichia coli* sulfite reductase,[2] in which an Fe_4S_4 cluster is coupled to siroheme through a Cys·S bridge, and the A and C clusters of *Clostridium thermoaceticum* carbon monoxide dehydrogenase (CODH), where an Fe_4S_4 cluster is connected by an unknown bridge(s) to a nickel site.[3] Although not demonstrated by protein crystallography, there is reasonable evidence that the assimilatory sulfite reductase from *Desulfovibrio vulgaris* contains the sulfide-bridged assembly Fe_4S_4−S-siroheme.[4] The remaining examples are found with the clusters of nitrogenase.[5−7] The P cluster consists of two cuboidal Fe_4S_3 units connected through a μ_m-S atom and two Cys·S bridges, with bridging multiplicity *m* dependent on the oxidation level of the Fe_8S_7 core.[7] The cofactor cluster (FeMoco) is constructed of $MoFe_3S_3$ and Fe_4S_3 cuboidal fragments bridged by three Fe−S−Fe interactions in a core of composition $MoFe_7S_9$. On the basis of EXAFS results, it is probable that vanadium-containing nitrogenase has an analogous structure.[8] It remains to be seen if other native iron−sulfur clusters with nuclearity exceeding that of the familiar Fe_4S_4 cubane-type clusters—most notably, the putative "prismane" Fe_6S_6 cluster[9]—are bridged assemblies or tightly integrated units.

Synthesis of bridged metal assemblies containing metal−sulfur clusters for the purpose of physicochemical and reactivity investigations provides a significant challenge, in considerable part because the fragments to be bridged are usually not identical. Fe_4S_4−(μ-SR)$_2$−Ni bridges have been constructed as an initial structural version of a CODH cluster.[10] In this case, one or two preformed tetradentate Ni(II) aminothiolate complexes displaced iodide from $[Fe_4S_4I_4]^{2-}$ to afford the product assembly. Thus far, representations of the sulfite reductase site in the form of Fe_4S_4−S−heme assemblies have been achieved with the heme group in the normal porphyrin oxidation state[11] or at the physiological isobacteriochlorin oxidation level.[12] In both cases, new reactions had to be

[⊗] Abstract published in *Advance ACS Abstracts,* August 15, 1997.

(1) Holm, R. H. *Pure Appl. Chem.* **1995**, *67*, 217.
(2) Crane, B. R.; Siegel, L. M.; Getzoff, E. D. *Science* **1995**, *270*, 59.
(3) (a) Ragsdale, S. W.; Kumar, M. *Chem. Rev.* **1996**, *96*, 2515. (b) Hu, Z.; Spangler, N. J.; Anderson, M. E.; Xia, J.; Ludden, P. W.; Lindahl, P. A.; Münck, E. *J. Am. Chem. Soc.* **1996**, *118*, 830.
(4) (a) Huynh, B. H.; Ling, K.; DerVartanian, D. V.; Peck, H. D., Jr.; LeGall, J. *J. Biol. Chem.* **1984**, *259*, 15373. (b) Tan, J.; Cowan, J. A. *Biochemistry* **1991**, *30*, 8910.
(5) Chan, M. K.; Kim, J.; Rees, D. C. *Science* **1993**, *260*, 792.
(6) Howard, J. B.; Rees, D. C. *Chem. Rev.* **1996**, *96*, 2965.
(7) Peters, J. W.; Stowell, M. H. B.; Soltis, S. M.; Finnegan, M. G.; Johnson, M. K.; Rees, D. C. *Biochemistry* **1997**, *36*, 1181.
(8) Eady, R. R. *Chem. Rev.* **1996**, *96*, 3013 and references therein.
(9) (a) Marritt, S. J.; Farrar, J. A.; Breton, J. L. J.; Hagen, W. R.; Thomson, A. J. *Eur. J. Biochem.* **1995**, *232*, 501. (b) de Vocht, M. L.; Kooter, I. M.; Bulsink, Y. B. M.; Hagen, W. R.; Johnson, M. K. *J. Am. Chem. Soc.* **1996**, *118*, 2766.
(10) (a) Osterloh, F.; Saak, W.; Haase, D.; Pohl, S. *J. Chem. Soc., Chem. Commun.* **1996**, *777*. (b) Osterloh, F.; Saak, W.; Pohl, S. *J. Am. Chem. Soc.* **1997**, *119*, 5648.
(11) Cai, L.; Holm, R. H. *J. Am. Chem. Soc.* **1994**, *116*, 7177.

S0002-7863(97)01401-7 CCC: $14.00

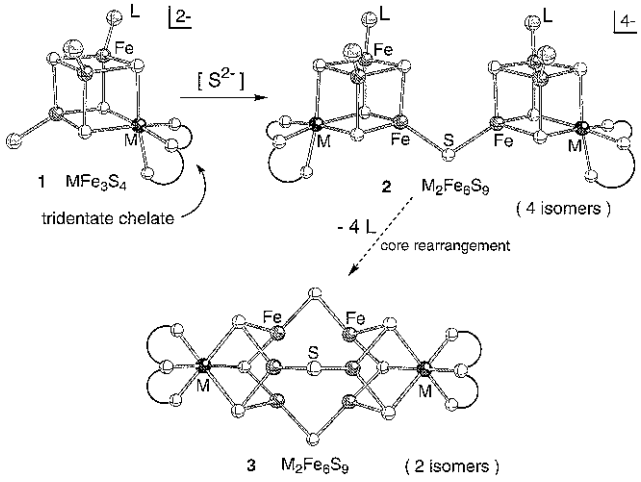

Figure 1. Conceptual scheme for a synthesis of the iron−molybdenum cofactor of nitrogenase involving the sulfide-bridged double cubane **2**. The number of isomers refers to molecules **2** and **3** in which the M site does not have trigonal symmetry, as shown.

developed for these unsymmetrical sulfide-bridged assemblies, a problem that is inherent to the synthesis of FeMoco with its different fragments and single-atom bridges.[13] Here an initial approach leading to symmetrically bridged assemblies may be more practical. Further, in the absence of the desired cuboidal fragments,[14] another tactic based on known clusters susceptible to one or more of the subsequent reactions of bridge formation and structural rearrangement may be entertained.

The cofactor core may be written as $M_2Fe_6S_9$, where M = Mo/V + Fe in the native state and M = Mo/V or Fe in conceivable symmetrized synthetic versions. Elsewhere, we have depicted the eight known structural types of bridged heterometal MFe_3S_4 double cubanes.[15] All but one utilize one or more bridge bonds involving M = V or Mo and thus are unsuitable for conversion into a cofactor-like structure. We are currently examining the conceptual reaction scheme in Figure 1. Single cubane **1**, constrained from forming bridge bonds at the M = Fe, V, or Mo site by a tight tridentate ligand or equivalent device, is converted to sulfide-bridged **2** by reaction at tetrahedral iron sites, whose substitutional lability is well-documented.[16,17] Ligand loss and induced core rearrangement recovers the FeMoco core structure **3**. The cores of **2** and **3** are isomers. This procedure depends on the formation of the double cubane **2**, preferably as an isolated intermediate. Two precedents exist for this cluster type. The initial example was provided by reaction 1 in DMF.[18,19] The product cluster could not be obtained as diffraction-quality crystals. However, structure **2** was demonstrated by ^{1}H NMR and the regiospecific reactivity engendered by the [1:3] site-differentiated precursor cluster. Reaction 2 resulted in a crystalline product whose μ_2-S

$$2[Fe_4S_4(LS_3)Cl]^{2-} + Li_2S \rightarrow \{[Fe_4S_4(LS_3)]_2S\}^{4-} + 2LiCl \quad (1)$$

$$2[Fe_4S_4Cl_4]^{2-} + Li_2S \rightarrow \{[Fe_4S_4Cl_3]_2S\}^{4-} + 2LiCl \quad (2)$$

double cubane structure was proven by an X-ray structure determination.[20] In addition to reactions 1 and 2, there is strong evidence for the formation in solution of the clusters Fe_4S_4−X−Fe_4S_4 with X = O^{2-}/OH^- and Se^{2-}, utilizing [1:3] site-differentiated precursor clusters.[16] These precedents raise the possibility of a new family of cubane-type clusters, essentially uninvestigated, in which component clusters are connected through a single-atom bridge. In the course of pursuing the scheme in Figure 1, we found it necessary to develop means of synthesis and characterization of sulfide-bridged double cubanes, especially of type **2**. The results of our first phase of investigation of this problem are reported here.

Experimental Section[19]

Preparation of Compounds. All operations and manipulations were performed under a pure dinitrogen atmosphere. Solvents were purified as appropriate and degassed prior to use. Compounds were identified by ^{1}H NMR, mass spectrometry, and, in certain cases, by crystallography and electrochemistry.

A. Single Cubane Clusters. $(Et_4N)_3[(Meida)VFe_3S_4Cl_3]$. A solution of 0.543 g (1.34 mmol) of $(Et_4N)_2$(Meida)[21] in 5 mL of Me_2SO was added to 1.00 g (1.34 mmol) of $(Me_4N)[(DMF)_3VFe_3S_4Cl_3]$[22] dissolved in 12 mL of Me_2SO. The reaction mixture was stirred for 30 min, treated with 100 mL of THF, and filtered, affording the mixed cation salt of the product cluster as a black powder. This material was washed with ether and dried in vacuo. To a solution of 0.300 g (0.32 mmol) of $(Me_4N)(Et_4N)_2[(Meida)VFe_3S_4Cl_3]$ in 100 mL of acetonitrile was added 53.3 mg (0.32 mmol) of Et_4NCl. The mixture was stirred overnight and filtered, and 100 mL of ether was layered onto the filtrate. The product was isolated by filtration and dried in vacuo to afford the product as 240 mg (72%) of a black crystalline solid. IR (KBr): ν_{COO} 1649 (s), 1610 (s) cm^{-1}. ^{1}H NMR (CD_3CN, anion): δ 14.9 (H_a), 6.01 (H_b). (The N-Me resonance was not located.) This compound was further identified by an X-ray structure determination.

$(Et_4N)_3[(Meida)VFe_3S_4(O$-$p$-$C_6H_4Me)_3]$. A solution of 0.480 g (0.486 mmol) of $(Et_4N)_3[(Meida)VFe_3S_4Cl_3]$ in 50 mL of acetonitrile was treated with 0.190 g (1.46 mmol) of p-MeC_6H_4ONa as a suspension in 25 mL of acetonitrile. The reaction mixture was stirred overnight and filtered, and the volume of the filtrate was reduced by *ca*. one-third in vacuo. An equal volume of ether was layered onto the filtrate. Dark brown needlelike crystals were collected by filtration and dried in vacuo to give 0.45 g (77%) of product. IR (KBr): ν_{COO} 1633 (s), 1603 (s) cm^{-1}. ^{1}H NMR (CD_3CN, anion): δ 18.6 (m-H′), 15.7 (p-Me′), 14.2 (m-H″), 10.7 (p-Me″), 5.44 (H_b), −1.04 (o-H″), −5.79 (o-H′). (The N-Me and H_a signals were not located.) This compound was further identified by an X-ray structure determination.

$(Et_4N)_2[(Meida)MoFe_3S_4Cl_3]$. This compound has been previously prepared.[23] The following procedure leads to a significantly higher yield. $(Et_4N)_2[(Cl_4cat)(MeCN)MoFe_3S_4Cl_3]$ was prepared by the reaction of $(Et_4N)_4[(Cl_4cat)_2Mo_2Fe_6S_8(SEt)_6]$[24] with benzoyl chloride in acetonitrile using an established procedure[17] and was isolated as black microcrystals in 90% yield. To a solution of 1.94 g (1.86 mmol) of

(12) Zhou, C.; Cai, L.; Holm, R. H. *Inorg. Chem.* **1996**, *35*, 2767.
(13) It is improbable that the complex structures of the metal clusters in nitrogenase can be reached in systems relying solely on spontaneous self-assembly.
(14) Cuboidal Fe_4S_3 clusters are known, but in the form $[Fe_4S_3(NO)_4(PR_3)_3]$, which has not proven useful for further chemical manipulation: Scott, M. J.; Holm, R. H. *Angew. Chem., Int. Ed. Engl.* **1993**, *32*, 564. Goh, C.; Holm, R. H. *Inorg. Chim. Acta*, in press.
(15) Huang, J.; Goh, C.; Holm, R. H. *Inorg. Chem.* **1997**, *36*, 356 and references therein.
(16) (a) Weigel, J. A.; Holm, R. H. *J. Am. Chem. Soc.* **1991**, *113*, 4184. (b) Zhou, C.; Holm, R. H. *Inorg. Chem.* **1997**, *36*, in press.
(17) Palermo, R. E.; Holm, R. H. *J. Am. Chem. Soc.* **1983**, *105*, 4310.
(18) Stack, T. D. P.; Carney, M. J.; Holm, R. H. *J. Am. Chem. Soc.* **1989**, *111*, 1670.
(19) Abbreviations: cat = catecholate(2−); Cl_4cat = tetrachlorocatecholate(2−); ESMS = electrospray mass spectrometry; FAB-MS = fast-atom-bombardment mass spectrometry; $(HBpz_3)^{1-}$ = hydrotris(pyrazolyl)borate(1−); Ida = imidodiacetate(2−); LS_3 = 1,3,5-tris((4,6-dimethyl-3-mercaptophenyl)thio)-2,4,6-tris(*p*-tolylthio)benzenate(3−); Meida = *N*-methylimidodiacetate(2−).
(20) Challen, P. R.; Koo, S.-M.; Dunham, W. R.; Coucouvanis, D. *J. Am. Chem. Soc.* **1990**, *112*, 2455.
(21) Zhou, J.; Hu, Z.; Münck, E.; Holm, R. H. *J. Am. Chem. Soc.* **1996**, *118*, 1966.
(22) Kovacs, J. A.; Holm, R. H. *Inorg. Chem.* **1987**, *26*, 702, 711.
(23) Demadis, K. D.; Coucouvanis, D. *Inorg. Chem.* **1995**, *34*, 436.
(24) Palermo, R. E.; Singh, R.; Bashkin, J. K.; Holm, R. H. *J. Am. Chem. Soc.* **1984**, *106*, 2600.

Table 1. Crystallographic Data[a] for $(Et_4N)_3[(Meida)VFe_3S_4Cl_3]\cdot CH_3CN$ (I), $(Et_4N)_3[(Meida)VFe_3S_4(O\text{-}p\text{-}C_6H_4CH_3)_3]$ (II), $(Et_4N)_4\{[Fe_4Se_4(LS_3)]_2Se\}\cdot 0.75THF\cdot 4DMSO$ (III), and $\{[VFe_4S_4(PEt_3)_4]_2S\}\cdot Et_2O$ (IV)

	I	II	III	IV
formula	$C_{31}H_{70}Cl_3Fe_3N_5O_4S_4V$	$C_{50}H_{88}Fe_3N_4O_7S_4V$	$C_{145}H_{221}Fe_8N_4O_{4.75}S_{22}Se_9$	$C_{52}H_{130}Fe_8OP_8S_{13}V_2$
formula wt	1030.01	1203.97	3880.18	1984.84
T, K	213	213	213	223
crystal system	orthorhombic	orthorhombic	triclinic	triclinic
space group	$Pna2_1$	$Pna2_1$	$P\bar{1}$	$P\bar{1}$
Z	4	4	2	2
a, Å	18.2910(8)	23.899(4)	18.9754(3)	14.200(6)
b, Å	13.5142(6)	20.101(6)	19.4617(3)	17.10(1)
c, Å	20.0329(9)	12.370(4)	49.5694(1)	19.133(7)
α, (deg)			90.4752(9)	95.32(4)
β, (deg)			91.1262(6)	101.81(3)
γ, (deg)			114.636(1)	101.50(4)
V, Å^3	4951.9(4)	5942(3)	16595(4)	4414(4)
d_{calc}, g/cm^3	1.382	1.346	1.575	1.487
w*R*2[b], *R*1[c]	0.1454, 0.0618	0.1698, 0.0886	0.2960, 0.1324	0.1320, 0.0527

[a] Obtained with graphite-monochromatized Mo Kα (λ = 0.710 73 Å) radiation. [b] $wR2 = \{\sum[w(F_o^2 - F_c^2)^2]/\sum[w(F_o^2)^2]\}^{1/2}$. [c] $R1 = \sum||F_o| - |F_c||/\sum|F_o|$.

$(Et_4N)_2[(Cl_4cat)(MeCN)MoFe_3S_4Cl_3]$ in 20 mL of DMF was added 0.274 g (1.86 mmol) of solid H_2Meida. The mixture was stirred at 55 °C overnight, cooled to room temperature, and filtered. Upon addition of 200 mL of ether to the filtrate, a dark sticky solid precipitated. The almost colorless supernatant was decanted, and the dark brown residue was washed with ether and extracted with 50 mL of acetonitrile. The extract was taken to dryness in vacuo, leading to 1.56 g (93%) of product as a dark brown microcrystalline solid. IR (KBr): ν_{COO} 1670 (s), 1644 (s) cm^{-1}. FAB-MS (*m*/*z*): 644 ($M^{2-}\cdot H^+$), 773 ($M^{2-}\cdot Et_4N^+$). ^{1}H NMR (Me_2SO): δ 14.9 (H_a), 5.85 (H_b). (The N-Me resonance was not located.)

$(Et_4N)_2[(Ida)MoFe_3S_4Cl_3]$. This compound was obtained by a procedure similar to the preceding preparation. The reaction of 0.194 g (0.186 mmol) of $(Et_4N)_2[(Cl_4cat)(MeCN)MoFe_3S_4Cl_3]$ with 24.7 mg (0.186 mmol) of solid H_2Ida produced 0.152 g (92%) of product as a dark brown crystalline solid. IR (KBr): ν_{COO} 1665 (s), 1640 (s) cm^{-1}. FAB-MS (*m*/*z*): 630 ($M^{2-}\cdot H^+$), 759 ($M^{2-}\cdot Et_4N^+$). ^{1}H NMR (Me_2SO): δ 14.4 (H_a), 5.65 (H_b). (The N−H resonance was not located.)

$(Et_4N)_2[(Meida)MoFe_3S_4(O\text{-}p\text{-}C_6H_4Me)_3]$. To a solution of 0.100 g (0.110 mmol) of $(Et_4N)_2[(Meida)MoFe_3S_4Cl_3]$ in 5 mL of acetonitrile was added 43 mg (0.33 mmol) of solid *p*-MeC_6H_4ONa. The reaction mixture was stirred overnight and filtered. Addition of 20 mL of ether to the filtrate caused the separation of a dark brown microcrystalline solid. This material was collected by filtration, washed with ether, and dried in vacuo to give the product as 110 mg (89%) of a dark brown solid. IR (KBr): ν_{COO} 1649 (s) cm^{-1}. ^{1}H NMR (CD_3CN): δ 20.1 (*m*-H′), 18.4 (*p*-Me′), 15.2 (*m*-H″), 13.6 (H_a), 12.8 (*p*-Me″), 5.21 (H_b), −3.23 (*o*-H″), −9.50 (*o*-H′).

$(Et_4N)_2[(Meida)MoFe_3S_4(SR)_3]$ (R = Et, *p*-C_6H_4F). To a solid mixture of 0.300 g (0.330 mmol) of $(Et_4N)_2[(Meida)MoFe_3S_4Cl_3]$ and 3 equiv of NaSR was added 15 mL of acetonitrile. The mixture was stirred for 4 h and filtered. Addition of 100 mL of ether to the greenish-brown filtrate resulted in the separation of a dark brown microcrystalline solid, which was collected by filtration, washed with ether, and dried in vacuo to afford the pure product in ca. 85% yield. IR (KBr): ν_{COO} 1649 (s), 1629 (s) (R = Et), 1652 (s), 1638 (s) (R = *p*-C_6H_4F) cm^{-1}. ^{1}H NMR (CD_3CN, R = Et, anion): δ 87.4 (*m*′-CH_2), 43.4 (*m*″-CH_2), 7.09 (*m*′-Me), 4.00 (*m*″-Me), 11.4 (H_a), 5.00 (H_b). ^{1}H NMR (CD_3CN, R = *p*-C_6H_4F, anion): δ 16.3 (*m*′−H), 11.8 (*m*″-H), 11.4 (H_a), 5.10 (H_b), 0.0 (*o*″-H), −6.2 (*o*′-H). ^{19}F NMR (MeCN): δ −80.9 (*m*′), −99.5 (*m*″).

B. Sulfido-Bridged Double Cubane Clusters. $(Bu_4N)_2\{[Fe_4S_4(LS_3)]_2S\}$. A solution of 73 mg (40 μmol) of $(Bu_4N)_2[Fe_4S_4(LS_3)Cl]$[16b,25] in 20 mL of acetonitrile was treated with 1.6 mg (20 μmol) of anhydrous Na_2S dissolved in a minimal volume of methanol. The reaction mixture was stirred overnight, and the solvent was removed in vacuo. The dark brown residue was extracted with a minimal volume of acetonitrile. The extract was filtered twice through Celite to remove NaCl and reduced to dryness in vacuo to afford the product as 67 mg (93%) of a dark brown solid. ^{1}H NMR (CD_3CN, anion): δ 8.66 (5-H), 7.22 (2′-H), 5.80 (3′-H), 4.53 (6-Me), 4.10 (4-Me), 2.27 (4′-Me). This spectrum is very similar to that of the Ph_4P^+ salt in Me_2SO.[18] (The ligand numbering scheme for this and the following cluster is given elsewhere.[16,18])

$(Bu_4N)_2\{[Fe_4Se_4(LS_3)]_2Se\}$. A solution of 47 mg (24 μmol) of $(Bu_4N)_2[Fe_4Se_4(LS_3)Cl]$[16b,25] in 12 mL of acetonitrile was treated with 1.1 mg (12 μmol) of Li_2Se[26] dissolved in a minimal volume of methanol. The procedure in the preceding preparation was followed, resulting in 41 mg (87%) of product as a dark brown solid. ^{1}H NMR (CD_3CN, anion): δ 8.87 (5-H), 7.11 (2′-H), 6.64 (3′-H), 5.12 (2-H), 4.61 (6-Me), 4.49 (4-Me), 2.24 (4′-Me). This compound was further identified by an X-ray structure determination.

$\{[VFe_4S_6(PEt_3)_4]_2S\}$. A solution of 0.20 g (0.21 mmol) of $[VFe_4S_6(PEt_3)_4Cl]$[27] in 20 mL of acetonitrile was treated with 5.6 mg (0.12 mmol) of Li_2S dissolved in a minimal volume (*ca*. 0.5 mL) of methanol. The reaction mixture was stirred overnight, and the solvent was removed in vacuo. The black residue was extracted with 200 mL of ether and the extract filtered. Slow evaporation of the solvent caused separation of the product as 57 mg (28%) of a highly crystalline black solid. ^{1}H NMR (C_6D_6): δ 2.53 (V-PCH_2), 1.61 (V-PCH_2CH_3), 0.46 (Fe-PCH_2CH_3), −4.69 (Fe-PCH_2). This compound was further identified by ESMS and an X-ray structure determination.

$(Et_4N)_4[((Meida)MoFe_3S_4Cl_2)_2S]\cdot 2LiCl$. To a solution of 0.240 g (0.260 mmol) of $(Et_4N)_2[(Meida)MoFe_3S_4Cl_3]$ in 5 mL of acetonitrile was added 6.1 mg (0.13 mmol) of solid Li_2S. The mixture gradually developed a dark brown precipitate upon vigorous stirring, which was continued overnight. This material was collected by filtration, thoroughly washed with acetonitrile, and dried in vacuo to give 0.150 g (64%) of product as a dark brown solid. IR (KBr): ν_{COO} 1639 (s) cm^{-1}. ^{1}H NMR (Me_2SO, anion): δ 21.0, 20.2, 20.0, 17.2, 16.7, 16.6 (H_a), 6.95, 6.25 (H_b), −3.6 (br, N-Me). Anal. Calcd for $C_{42}H_{94}Cl_6Fe_6Li_2Mo_2N_6O_8S_9$: C, 27.22; H, 5.11; Cl, 11.48; Fe, 18.08; Mo, 10.35; N, 4.53; S, 15.57. Found: C, 27.08; H, 5.03; Cl, 11.32; Fe, 18.15; Mo, 10.28; N, 4.65; S, 15.65. This compound was further identified by ESMS.

X-ray Structure Determinations. Structures were determined for the four compounds listed in Table 1. Single crystals of I, II, and IV were taken from the reaction products. A (marginally) suitable crystal of III was obtained as a decomposition product of $(Et_4N)_3[Fe_3Se_4(LS_3)]$[21] in Me_2SO solution into which THF and ether were diffused; crystals appeared after *ca*. 1 month. Crystals were coated with Apiezon L grease, attached to glass fibers, transferred to either a Nicolet P3F (IV) or a Siemens SMART CCD diffractometer (all others), and cooled in a dinitrogen stream to either −50 °C (IV) or −60 °C (all others). Lattice parameters were obtained from least-squares analysis of more than 25 machine-centered reflections. The raw intensity data (including corrections for scan speed, background, and Lorentz and polarization effects) were converted to structure factor amplitudes and their esd's

(25) Stack, T. D. P.; Weigel, J. A.; Holm, R. H. *Inorg. Chem.* **1990**, *29*, 3745.

(26) Gladysz, J. A.; Hornby, J. L.; Garbe, J. E. *J. Org. Chem.* **1978**, *43*, 1204.

using the program XDISK (IV) or SAINT (all others). None of the compounds showed significant decay over the course of data collection. Absorption corrections were applied using the program SADABS except for structure IV which was corrected using XABS2. Space group assignments were based on analysis of systematic absences, *E* statistics, and successful refinement of the structures. The final resolution for all structures was 0.90 Å^3. Structures were solved by direct methods with the aid of successive difference Fourier maps using the SHELXS-90 program, and were refined by the least-squares method on F^2 using SHELXTL-93, incorporated into the SHELXTL-PC V 5.03 suite. All non-hydrogen atoms were refined anisotropically. Hydrogen atoms were not included for the disordered ether molecules in IV. All other hydrogen atoms were assigned to ideal positions and refined using a riding model with an isotropic thermal parameter 1.2× that of the attached carbon atom (1.5× for methyl hydrogens).

The asymmetric unit of I consists of one anion, three cations, and one acetonitrile solvate molecule. The asymmetric unit of II contains one anion and three cations, while that of III includes two independent cluster anions and eight cations, one of which was severely disordered, requiring that its position be constrained. Also present were eight Me_2SO molecules, all of which were disordered and required constraints, and 1.5 THF molecules. One of the THF molecules was severely disordered and was refined at one-half occupancy. Several peaks of electron density (above 1 e$^-$/Å^3) in the vicinity of the disordered cation could not be modeled effectively. The large R_1 and wR_2 residual factors are due to minimal crystal quality. The asymmetric unit of IV consists of one cluster and one ether solvate molecule. One of the triethylphosphine ligands on the cluster was highly disordered. Attempts to model this disorder were unsuccessful, resulting in two peaks of electron density (above 1 e$^-$/Å^3) near the carbon atoms of ethyl arms of the ligand. The ether molecule was refined over two positions, each of which refined successfully in one-half occupancy. One of the ether oxygen atoms was positioned directly on a 2-fold axis while the other had an oxygen and a carbon atom in half-occupancy split across a 2-fold axis. Crystallographic data are listed in Table 1. In the last cycles of refinement, all parameters shifted by less than 1% of their esd's and the final difference Fourier maps showed no significant electron density except where previously noted.[28]

Other Physical Measurements. All measurements were performed under anaerobic conditions. ^{1}H NMR spectra were obtained using a Bruker AM-500 and AM-400 spectrometers. Electrochemical measurements were performed with a PAR Model 263 potentiostat/galvanostat using a Pt working electrode and 0.1 M (Bu_4N)(PF_6) supporting electrolyte. Potentials are referenced to the SCE. FAB mass spectra were measured on a JEOL SX-102 instrument using 3-nitrobenzyl alcohol as the matrix. Electrospray mass spectra were recorded using a Platform 2 mass spectrometer (Micromass Instruments, Danvers, MA). Samples (ca. 50 μM) were introduced at a flow rate of 3 mL/min from a syringe pump (Harvard Apparatus). The electrospray probe capillary was maintained at a potential of 3.0 kV (−3.0 kV for negative ion measurements) and the orifice to the skimmer potential (cone voltage) was varied from 10 to 40 V, as appropriate for each measurement. Spectra were collected in the multichannel acquisition mode; spectra were acquired at 5 s/scan, and 12 scans were accumulated for each spectrum.

Results and Discussion

The following single cubane (**4**−**10**) and double cubane (**11**−**15**, **17**) clusters are of primary interest in this investigation. Of these, **6**, **11**, and **12** have been reported previously; the remainder are new species, all of which have been isolated.

Sulfide- and Selenide-Bridged Double Cubanes. (a) Preparation and Structure. We initiated an investigation of these cluster types in order to develop criteria, apart from X-ray crystal structures, for the formation of bridged double cubanes. Reaction 1 has been repeated under different conditions than previously,[18] and cluster **12** as its Bu_4N^+ salt, pure by an ^{1}H NMR criterion, were isolated in 93% yield. Formation of a bridged structure is indicated by the appearance of an NMR spectrum with isotropic shifts substantially larger than those of the single cubanes $[Fe_4S_4(LS_3)L']^{2-}$ with L′ = RS$^-$ and HS$^-$.[16,18] For example, in acetonitrile the 5-H resonance of the coordinating arm of the tridentate LS_3 ligand incorporated into **12** appears at 8.66 ppm whereas the 5-H shifts of both $[Fe_4S_4(LS_3)(SMe)]^{2-}$ [16b] and $[Fe_4S_4(LS_3)(SH)]^{2-}$ [18] are 8.16 ppm. This amounts to a 35% larger isotropic shift in **12** compared to the single cubanes. Despite numerous attempts, we have been unable to obtain diffraction-quality crystals of a salt of **12**. As a result, reaction 3, affording the analogous selenide-bridged double cubane **13**, was examined.

$$2[Fe_4Se_4(LS_3)Cl]^{2-} + Li_2Se \rightarrow \{[Fe_4Se_4(LS_3)]_2Se\}^{4-} + 2LiCl \quad (3)$$

The ^{1}H NMR properties of **13** are analogous to those of **12**, with its 5-H isotropic shift being 27% larger than that of $[Fe_4Se_4(LS_3)(SMe)]^{2-}$.[16b] Further, the 5-H isotropic shift of **13** is 11% larger than that of **12**, consistent with usual property of larger isotropic shifts for selenide vs sulfide clusters because of the smaller antiferromagnetic coupling and larger paramagnetism of the $[Fe_4Se_4]^{2+}$ core. These properties have been documented at length elsewhere.[16b] In a related study of the stability of the cuboidal cluster $[Fe_3Se_4(LS_3)]^{3-}$,[21] we observed slow decomposition in Me_2SO solution. Diffusion of ether and THF into this solution resulted in the crystallization of a solvated salt of **13** (compound III, Table 1), identified by an X-ray structure determination. Because superior crystals were not obtained from reaction 3 despite our best efforts, we report the refined structure of the crystal for which data were collected. The asymmetric unit contains two complete cluster anions. The structure of one anion and its core are contained in Figure 2; the bridged double cubane arrangement is immediately apparent. Metric parameters are summarized in Table 2. Because the bond angles and distances in the individual cubanes are not significantly different from those in $[Fe_4Se_4]^{2+}$ single cubanes,[16b,18,29] ranges and mean values of selected distances are tabulated and angles are omitted.[28] In each double cubane, the LS_3 ligands have the conformations *ababab* and *ababaa*,[25] meaning that the coordinating arms and buttressing legs alternate in position

$[(Meida)VFe_3S_4Cl_3]^{3-}$ **4**

$[(Meida)VFe_3S_4(O\text{-}p\text{-}C_6H_4Me)_3]^{3-}$ **5**

$[(Meida)MoFe_3S_4Cl_3]^{2-}$ **6**[23]

$[(Ida)MoFe_3S_4Cl_3]^{2-}$ **7**

$[(Meida)MoFe_3S_4(O\text{-}p\text{-}C_6H_4Me)_3]^{2-}$ **8**

$[(Meida)MoFe_3S_4(SEt)_3]^{2-}$ **9**

$[(Meida)MoFe_3S_4(S\text{-}p\text{-}C_6H_4F)_3]^{2-}$ **10**

$[(Fe_4S_4Cl_3)_2(\mu_2\text{-}S)]^{4-}$ **11**[20]

$\{[Fe_4S_4(LS_3)]_2(\mu_2\text{-}S)\}^{4-}$ **12**[18]

$\{[Fe_4Se_4(LS_3)]_2(\mu_2\text{-}Se)\}^{4-}$ **13**

$\{[VFe_4S_6(PEt_3)_4]_2(\mu_2\text{-}S)\}$ **14**

$\{[(Meida)MoFe_3S_4Cl_2]_2(\mu_2\text{-}S)\}^{4-}$ **15**

$[(Meida)\ MoFe_3S_4Cl(\mu_2\text{-}S)]_n^{2n-}$ **16**

$\{[(Meida)MoFe_3S_4Cl_2](\mu_2\text{-}S)(Fe_4S_4Cl_3)\}^{4-}$ **17**

(27) Nordlander, E.; Lee, S. C.; Cen, W.; Wu, Z. Y.; Natoli, C. R.; Di Cicco, A.; Filipponi, A.; Hedman, B.; Hodgson, K. O.; Holm, R. H. *J. Am. Chem. Soc.* **1993**, *115*, 5549.

(28) See paragraph at the end of this article concerning Supporting Information.

Table 2. Selected Interatomic Distances (Å) and Angles (deg) for $\{[Fe_4Se_4(LS_3)]_2Se\}^{4-}$

		Bridge	
Anion 1		Anion 2	
Fe(11)−Se(1)	2.274(8)	Fe(31)−Se(2)	2.277(8)
Fe(21)−Se(1)	2.282(9)	Fe(41)−Se(2)	2.275(9)
Fe(11)−Se(1)−Fe(21)	115.5(4)	Fe(31)−Se(2)−Fe(41)	112.7(4)
		Core	
Fe−Se range	2.312(8)−2.397(8)	Fe−Se range	2.308(10)−2.381(8)
mean of 24	2.36(2)	mean of 24	2.36(2)
Fe−Fe range	2.690(9)−2.803(10)	Fe−Fe range	2.652(10)−2.801(10)
mean of 12	2.75(3)	mean of 12	2.74(4)
Fe−S range	2.21(2)−2.27(2)	Fe−S range	2.21(2)−2.24(2)
mean of 6	2.23(2)	mean of 6	2.22(1)

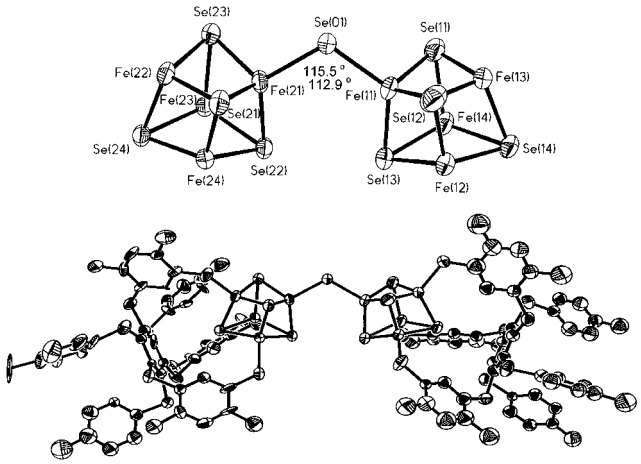

Figure 2. Structure of $\{[Fe_4Se_4(LS_3)]_2Se\}^{4-}$ showing one of the two inequivalent anions in its entirety (lower) and the core structure with 50% probability ellipsoids, the atom labeling scheme (anion 1), and Fe−Se−Fe bridge angles (upper). The individual cubane on the lower right has ligand conformation *abababa*, and that on the lower left has conformation *ababaa*.

above and below the central benzene ring in the first instance but an adjacent arm and leg are on the cluster side of this ring in the second. Individual $[Fe_4Se_4]^{2+}$ cores in the two clusters are unsystematically distorted from idealized cubic symmetry. Terminal Fe−S distances are in the normal range, but the mean values are somewhat less (0.03−0.04 Å) than in the two other $[Fe_4Se_4(LS_3)L']^{1-,2-}$ clusters of known structure.[16b,18]

Principal interest attends the bridge structure. The bridge bonds average over the two clusters to 2.277(4) Å. As would be expected for bonds involving μ_2-Se rather than μ_3-Se atom, bridge bonds are shorter than all core bonds, whose mean value is 2.36(2) Å in both clusters. Bridge angles are 115.5(4)° and 112.7(4)°, leading to Fe···Fe separations of 3.85 and 3.79 Å, respectively. Across the bridge, the cubanes in anion 1 are juxtaposed at the dihedral angles Se(13)−Fe(11)−Se(1)−Fe(21) = 20.7° and Se(22)−Fe(21)−Se(1)−Fe(11) = 27.2°, which are measures of the twist of the cubanes out of the Fe(11,21)-Se(1) bridge plane. The two cubanes are twisted out of alignment across the bridge by the angle Se(13)−Fe(11)−Fe(21)−Se(22) = 7.1°.

The corresponding angles in anion 2 are 17.0° and 21.9° and a bridge twist angle of 3.8°. This conformation places Se(13)···Se(22) at 3.74 Å in anion 1 and Se(31)···Se(41) at 3.67 Å in anion 2 as the closest intercubane distances. In anion 1, the core faces Fe(11,12)Se(12,13) and Fe(21,24)Se(21,22), containing the bridged iron atoms, are roughly opposite each other. Consequently, of the 12 Se−Fe−Se angles involving the two bridging iron atoms, the four largest involve Se(1) and Se(12,13,21,22) and occur in range 111.9(3)−121.9(3)°. Of these, the largest angle is Se(1)−Fe(11)−Se(13). All other angles at Fe(11,21) are in the interval 102.8(3)−108.1(3)°. A similar situation holds for anion 2, where the four largest angles are 111.9(3)−121.7(3)° and the remaining angles are in the range 104.4(3)−107.1(3)°. The bridge/cubane conformation and pattern of distortion of Se−Fe−Se angles at the bridging sites can only be ascribed to intercubane repulsion. For comparison, in the double cubane **11**, the individual cubanes are also twisted about the bridge bonds by a corresponding dihedral angle of 50.0° and the Fe−S−Fe bridge angle is 102.2°.[20]

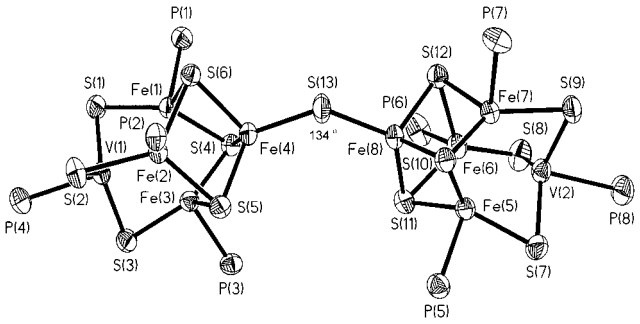

Figure 3. Structure of $[VFe_4S_6(PEt_3)_4]_2S$ showing 50% probability ellipsoids and the atom labeling scheme. Bond distances (Å): Fe(4)−S(13), 2.194(2); Fe(8)−S(13), 2.189(2); Fe(4)···Fe(8), 4.03 Å; Fe(4,8)−(μ_3-S), 2.26(1) (mean of 6). Bond angles (deg): Fe(4)−S(13)−Fe(8), 134.0(1); S(13)−Fe(μ_3-S), 110.1(1)−122.1(1) (range of 6). The individual clusters are further separated by the following distances: S(5)···(S11), 5.57 Å; S(6)···S(12), 6.98 Å; S(4)···S(10), 7.15 Å.

The clusters $[MFe_4S_6(PEt_3)_4L]$ (L = Cl^-, RS^-) contain the fragment $Fe_4(\mu_3\text{-}S)_3(\mu_2\text{-}S)_3$; therefore, they are the closest approaches to the FeMoco structure currently available.[27,30] Noting that the L = RS^- clusters can be prepared by thiolate displacement of chloride,[30] we examined the related reaction 4.

$$2[VFe_4S_6(PEt_3)_4Cl] + Li_2S \rightarrow [VFe_4S_6(PEt_3)_4]_2S + 2LiCl \quad (4)$$

While the product cannot be a double cubane, it does provide another case of an Fe−S−Fe bridge between clusters. The product is the sulfide-bridged assembly **14**, as demonstrated by the structure in Figure 3. The metric features of the individual clusters are unimportantly different from those of the single clusters $[VFe_4S_6(PEt_3)_4L]$ (L = Cl^-,[27] PhS^- [30]) and are not further considered. The mean Fe−S bridge distance is 2.192

(29) (a) Bobrik, M. A.; Laskowski, E. J.; Johnson, R. W.; Gillum, W. O.; Berg, J. M.; Hodgson, K. O.; Holm, R. H. *Inorg. Chem.* **1978**, *17*, 1402. (b) Fenske, D.; Maué, P.; Merzweiler, K. *Z. Naturforsch.* **1987**, *B42*, 928. (c) Rutchik, S.; Kim, S.; Walters, M. A. *Inorg. Chem.* **1988**, *27*, 1513. (d) Ahle, A.; Dehnicke, K.; Maichle-Mosmer, J.; Strähle, J. *Z. Naturforsch.* **1994**, *B49*, 434.

(30) Cen, W.; MacDonnell, F. M.; Scott, M. J.; Holm, R. H. *Inorg. Chem.* **1994**, *33*, 5809.

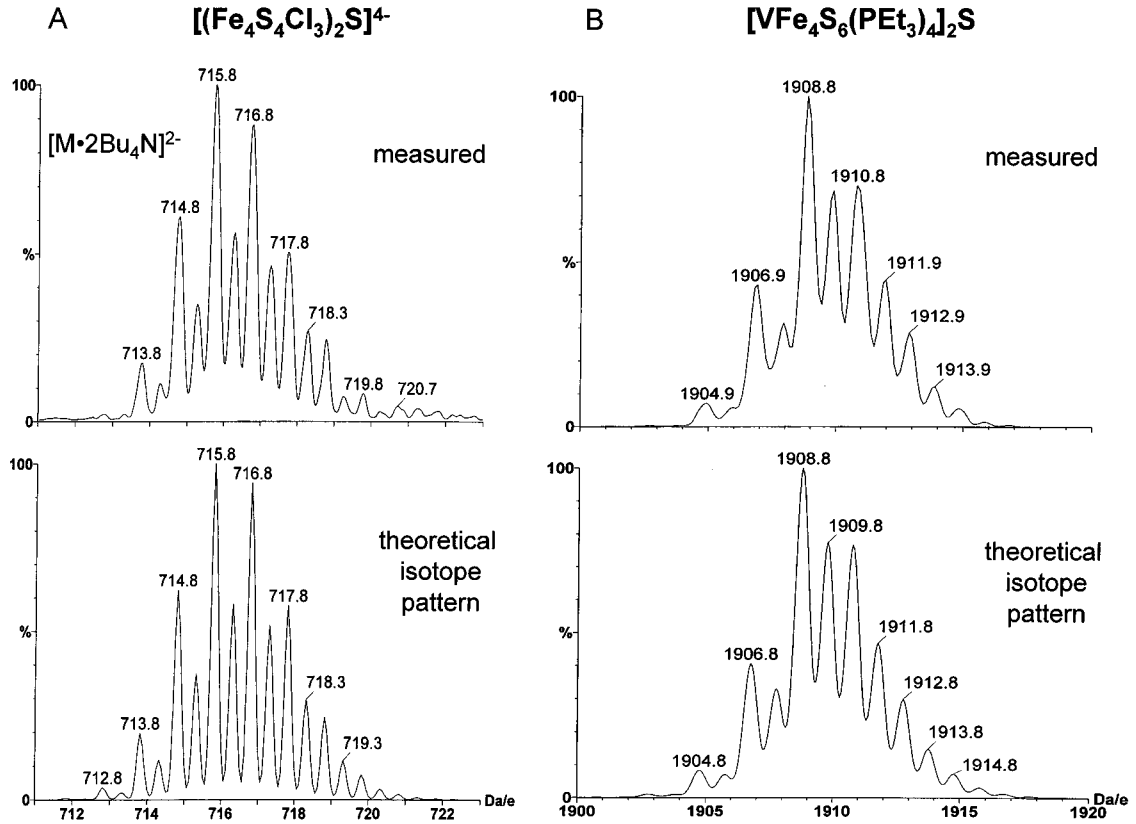

Figure 4. Measured negative-ion ESMS of $\{[Fe_4S_4Cl_3]_2S\cdot 2Bu_4N\}^{2-}$ (A) and positive-ion ESMS of $\{[VFe_4S_6(PEt_3)_4]_2S\cdot H\}^{1+}$ (B). Measured spectra are at the top and theoretical isotope patterns below. The compound $(Bu_4N)_4\{[Fe_4S_4Cl_3]_2S\}$ was sampled from an acetonitrile solution and $[VFe_4S_6(PEt_3)_4]_2S$ from a dichloromethane solution.

Å, essentially identical with that in **11** (2.206(4) Å[20]). The Fe−S−Fe bridge angle of 134.0(1)° is much larger than the corresponding angles in **11** and **13** and appears to arise from repulsions across the bridge involving the three Et_3P ligands on the individual clusters. Earlier we have demonstrated that Fe−S−Fe angles are "soft", being deformable by steric factors operating across the bridge.[31]

(b) Mass Spectrometry. With X-ray structural proof of the Fe−S−Fe bridge in **14** and the Fe−Se−Fe bridge in **13**, and NMR similarities between **12** and **13** leaving no doubt that the former has an Fe−S−Fe bridge, we sought alternate and more rapid means of establishing the presence of the $Fe_4Q_4-Q-Fe_4Q_4$ double cubanes (Q = S, Se) in solution without reliance on X-ray structures. Because of the probable fragility of Fe−Q−Fe bridges, unsupported by any additional ligation, we have turned to electrospray mass spectrometry. An advantageous feature of ESMS is the transfer of *existing* ions into the gas phase for analysis. The method has been profitably applied to metal clusters[32] and iron−sulfur proteins.[33] Two results are considered here. We have reinvestigated reaction 2 and isolated the products as Bu_4N^+ salts. The negative ion ESMS of $(Bu_4N)_4$[**11**] sampled in acetonitrile solution contains an intense feature centered near *m*/*z* 716. This is shown to correspond to $[\mathbf{11}\cdot 2Bu_4N]^{2-}$ by comparison of the observed spectrum with the theoretical isotope pattern in Figure 4A. In another experiment, the ESMS of **14** in dichloromethane was determined. An intense feature around *m*/*z* 1908 was observed. As shown in Figure 4B, the measured pattern corresponds to $[\mathbf{14}\text{-}H]^+$. These results demonstrate that clusters **11** and **14** maintain their integrity in solution. ^{1}H NMR demonstrates this behavior for **12** and **13**. ESMS is clearly useful in establishing cluster nuclearity of Fe−S−Fe double cubanes; additional examples follow.

(c) Voltammetry. Covalently bridged clusters whose component clusters are separated by ca. 4 Å or less usually show coupled redox steps. For heterometal MFe_3S_4 double cubanes, two or three bridging interactions connect the component cubanes. The classic examples of this type of behavior are the clusters $[M_2Fe_6S_8(SR)_9]^{3-}$ (M = Mo and W,[34] Re[35]) which contain $M(\mu_2\text{-}SR)_3M$ bridges and show fully reversible coupled redox reactions whose potentials are separated by *ca*. 200 mV. The question arises as to whether individual cubanes are sufficiently coupled by one single-atom bridge to manifest resolvable potentials. The voltammograms of **12** and **13** in acetonitrile, shown in Figure 5 (lower), reveal two discrete redox steps separated by 240−250 mV. Redox potentials for these and other clusters are set out in Table 3; the data include individual clusters for comparison. The clusters $[Fe_4Q_4(LS_3)(SEt)]^{2-}$ (Q = S, Se) show only a single reduction step in the same potential range. The potentials for **13** are 40−50 mV less negative than those for **12**, consistent with the behavior found upon substitution of sulfide with selenide in other clusters.[16b] We have never encountered an exception to this direction of potential shift in any pair of clusters. We next examined **14** in dichloromethane, in which medium the bridged structure was

(31) Mukherjee, R. N.; Stack, T. D. P.; Holm, R. H. *J. Am. Chem. Soc.* **1988**, *110*, 1850.

(32) (a) van den Bergen, A.; Colton, R.; Percy, M.; West, B. O. *Inorg. Chem.* **1993**, *32*, 3408. (b) Andersen, U. N.; McKenzie, C. J.; Bojesen, G. *Inorg. Chem.* **1995**, *34*, 1435.

(33) Pétillot, Y.; Forest, E.; Meyer, J.; Moulis, J.-M. *Anal. Biochem.* **1995**, *228*, 56.

(34) (a) Wolff, T. E.; Power, P. P.; Frankel, R. B.; Holm, R. H. *J. Am. Chem. Soc.* **1980**, *102*, 4694. (b) Christou, G.; Garner, C. D. *J. Chem. Soc., Dalton Trans.* **1980**, 2354. (c) Christou, G.; Mascharak, P. K.; Armstrong, W. H.; Papaefthymiou, G. C.; Frankel, R. B.; Holm, R. H. *J. Am. Chem. Soc.* **1982**, *104*, 2820.

(35) Ciurli, S.; Carrié, M.; Holm, R. H. *Inorg. Chem.* **1990**, *29*, 3493.

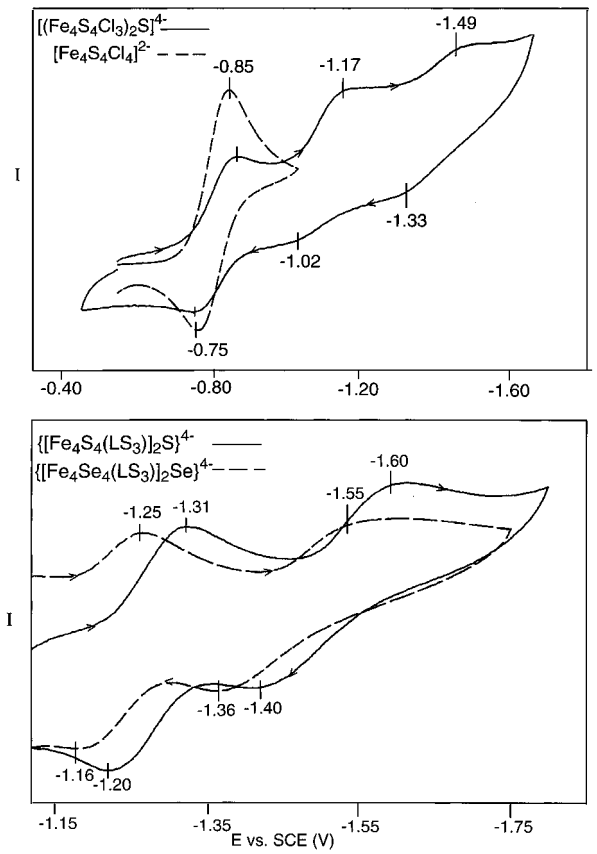

Figure 5. Cyclic voltammograms (100 mV/s) of $[Fe_4S_4Cl_4]^{2-}$ and $[(Fe_4S_4Cl_3)_2S]^{4-}$ (upper) and $\{[Fe_4Q_4(LS_3)]_2Q\}^{4-}$ (Q = S, Se) in acetonitrile (lower). Peak potentials are indicated.

Table 3. Redox Potentials of Clusters

cluster	solvent	$E_{1/2}$, V[a]
$[Fe_4S_4(LS_3)(SEt)]^{2-}$	MeCN	−1.12[b]
$\{[Fe_4S_4(LS_3)]_2S\}^{4-}$	MeCN	−1.26, −1.50
$[Fe_4Se_4(LS_3)(SEt)]^{2-}$	MeCN	−1.09[b]
$\{[Fe_4Se_4(LS_3)]_2Se\}^{4-}$	MeCN	−1.21, −1.46
$[Fe_4S_4Cl_4]^{2-}$	MeCN	−0.80
$[(Fe_4S_4Cl_3)_2S]^{4-}$	MeCN	−1.10, −1.41
$[VFe_4S_6(PEt_3)_4(SEt)]^{2-}$	MeCN	−0.05, −0.91[c]
$[VFe_4S_6(PEt_3)_4]_2S$	CH_2Cl_2	−0.09, −0.40[d]
		−0.99, −1.18[e]
$[(Ida)MoFe_3S_4Cl_3]^{2-}$	DMF	−0.84
$[(Meida)MoFe_3S_4Cl_3]^{2-}$	DMF	−0.81
$\{[(Meida)MoFe_3S_4Cl_2]_2S\}^{4-}$	DMF	−1.01, −1.34

[a] vs SCE, 297 K. [b] Reference 16b. [c] Reference 30. [d] Oxidation. [e] Reduction.

demonstrated by ESMS. The voltammogram in Figure 6 (upper) reveals two reductions and two oxidations separated by 190 and 310 mV, respectively. The individual cluster $[VFe_4S_6(PEt_3)_4(SEt)]$ shows only one reduction and one oxidation step. The first reductions of bridged clusters occur at more negative potentials than those of closely related individual clusters. With these results in hand, we decided to reexamine the products of reaction 2, for which this shift of potentials was not apparent from the reported data.[20]

A microcrystalline solid containing Bu_4N^+ salts, isolated from reaction 2 and used for ESMS (Figure 4A), was examined by cyclic voltammetry in acetonitrile. The result, reproduced in multiple experiments, is displayed in Figure 5 (upper). Three steps are observed, at $E_{1/2} = -0.80$, −1.10, and −1.41 V. The first two steps were previously attributed to double cubane **11**, and the third was not reported.[20] However, the −0.80 V feature is identical with that of precursor cluster $[Fe_4S_4Cl_4]^{2-}$, which

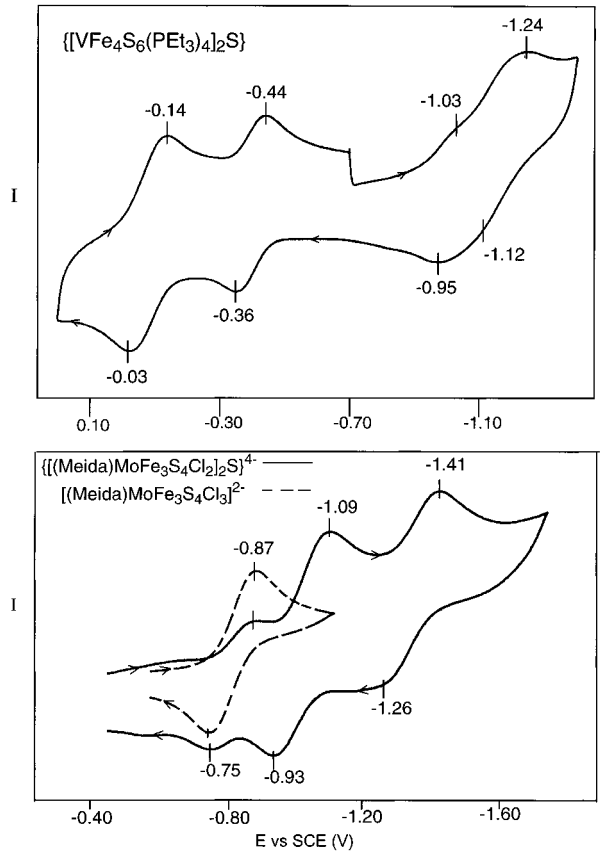

Figure 6. Cyclic voltammograms of $[VFe_4S_6(PEt_3)_4]_2S$ in dichloromethane at 100 mV/s (upper) and $[(Meida)MoFe_3S_4Cl_3]^{2-}$ and $\{[(Meida)MoFe_3S_4Cl_2]_2S\}^{4-}$ in Me_2SO at 400 mV/s (lower). Peak potentials are indicated.

was also detected in solution by ESMS. The remaining two steps, separated by 310 mV, are assigned to the coupled reductions of **11**. Consequently, there emerges for bridged clusters **11**−**14**, whose nearest metal atom distances across the bridges are 3.4−4.0 Å, the consistent behavior of coupled redox processes. For double cubanes, potentials of sequential reductions are separated by 240−310 mV. We take the coupled reactions and differences of potentials within or near this range as diagnostic of sulfide-bridged double cubanes. This behavior, together with ESMS, provides secure means of identifying such clusters in solution.

Molybdenum−Iron-Sulfide-Bridged Double Cubanes. Prosecution of the scheme in Figure 1 first requires the conversion of heterometal MFe_3S_4 cubane **1** to sulfide-bridged double cubane **2** with total core composition $M_2Fe_6S_9$. As observed earlier, the M = V or Mo site must be protected in order to subvert bridge formation at that site. Noting the formation of $[(Meida)Fe_4S_4(LS_3)]^{3-}$ [21] and, in particular, $[(Meida)MFe_3S_4Cl_3]^{2-}$,[23] we have utilized *fac*-tridentate Meida as the protecting ligand.

(a) Formation and Structure of VFe_3S_4 Single Cubanes. For VFe_3S_4 clusters, the Meida ligand is readily introduced at the vanadium site utilizing $[(DMF)_3VFe_3S_4Cl_3]^{1-}$ [22] as the precursor cluster. The reaction readily occurs in Me_2SO/THF solution at room temperature, affording $(Et_4N)_3$[**4**] in 72% yield. Related reactions of the $(DMF)_3V$ site have been demonstrated previously.[22,36,37] Treatment of the latter compound with 3 equiv of sodium *p*-cresolate in acetonitrile gave $(Et_4N)_3$[**5**] (77%).

(36) Ciurli, S.; Holm, R. H. *Inorg. Chem.* **1989**, *28*, 1685.
(37) Malinak, S. M.; Demadis, K. D.; Coucouvanis, D. *J. Am. Chem. Soc.* **1995**, *117*, 3126.

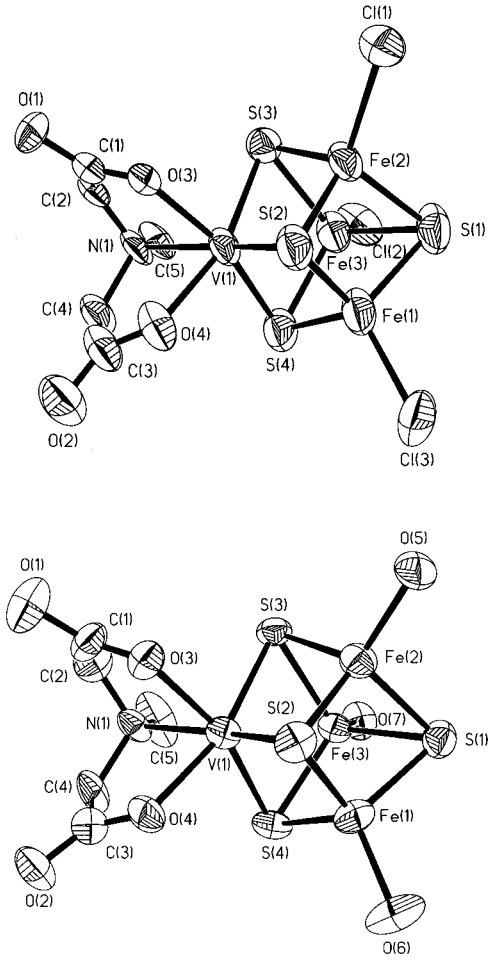

Figure 7. Structure of $[(Meida)VFe_3S_4Cl_3]^{3-}$ (upper) and $[(Meida)VFe_3S_4(O\text{-}p\text{-}C_6H_4CH_3)_3]^{3-}$ (lower), showing 50% probability ellipsoids and the atom labeling schemes.

These clusters were prepared in this work to demonstrate the formation and structure of the (Meida)V cluster fragment; reactions of **4** and **5** will be reported subsequently. Structure proof of the two clusters is presented in Figure 7, and selected metric details are summarized in Table 4. Because bond distances and angles of the $[VFe_3S_4]^{2+}$ cores are very similar to those of previously reported structures,[22,37] the tabulated data emphasize the vanadium sites.

These clusters have three important structural features. (i) The Meida ligand coordinates in the *fac* mode, forming distorted octahedral VS_3NO_2 coordination units. The distortions are somewhat different in the two clusters. (ii) Each cluster has idealized C_s symmetry, resulting in two types of iron sites. Using previous nomenclature,[17] these are m′ (Fe(3), in the mirror plane) and m″ (Fe(1,2), related by the plane). (iii) Each Meida ligand contains two equivalent methylene groups (under C_s symmetry), but the protons of each are diastereotopic (H_a, H_b). These features are evident in ^{1}H NMR spectra (cf. Experimental Section), which are isotropically shifted because of the $[VFe_3S_4]^{2+}$ cluster spin $S = {}^3/_2$.[38] In the spectrum of **4**, the H_a (14.9 ppm) and H_b (6.01) resonances are well-resolved. The spectrum of **5** contains two sets of *p*-tolyl signals in a 2:1 intensity ratio and H_b at 5.44 ppm; the H_a resonance is obscured by other signals. At ambient temperature, neither these clusters nor the isoelectronic $[MoFe_3S_4]^{3+}$ clusters **6**−**10** (vide infra) are fluxional. Thus, rigid tridentate binding by Meida provides the desired coordination saturation at the vanadium site.

(38) Carney, M. J.; Kovacs, J. A.; Zhang, Y.-P.; Papaefthymiou, G. C; Spartalian, K.; Frankel, R. B.; Holm, R. H. *Inorg. Chem.* **1987**, *26*, 719.

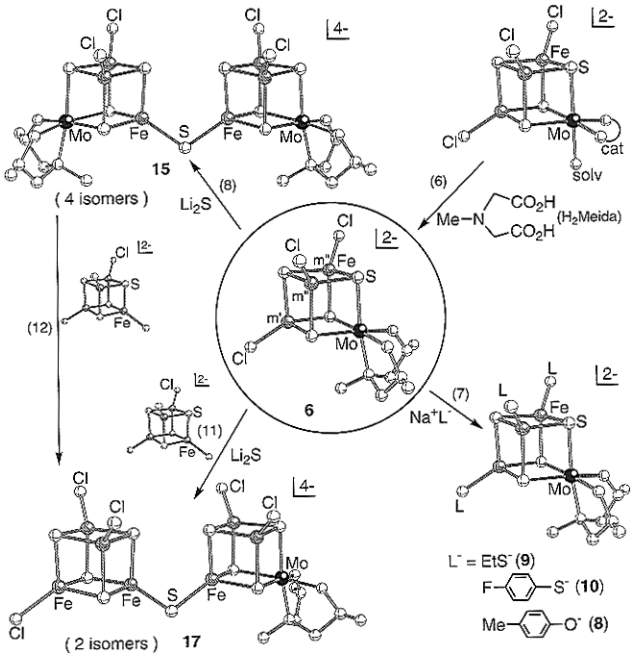

Figure 8. Reaction scheme showing the formation of single cubane **6** from $[(Cl_4cat)MoFe_3S_4Cl_3]^{2-}$ and H_2Meida, the conversion of **6** by chloride substitution to **8**−**10**, and the formation of symmetrical (**15**) and unsymmetrical (**17**) sulfide-bridged double cubanes. The additional cluster reactant in reactions 11 and 12 is $[Fe_4S_4Cl_4]^{2-}$; note that these reactions have additional products (see text).

(b) Formation of $MoFe_3S_4$ Single and Double Cubanes. (i) Reactions. These clusters are obtained by the reactions set out in Figure 8. No solvated analogue of $[(DMF)_3VFe_3S_4Cl_3]^{1-}$ exists in molybdenum cluster chemistry. The catecholate ligand exchange reaction 5[24] (L = RS^-, Cl^-; L′ = solv or other ligand) is the basis for introducing the Meida ligand into a $[MoFe_3S_4]^{3+}$ cluster by reaction 6. These clusters have $S = {}^3/_2$,[38] affording

$$[(cat)MoFe_3S_4L_3L']^{2-,3-} + *catH_2 \rightarrow [(*cat)MoFe_3S_4L_3L']^{2-,3-} + catH_2 \quad (5)$$

$$[(Cl_4cat)MoFe_3S_4Cl_3]^{2-} + H_2Meida \rightarrow [(Meida)MoFe_3S_4Cl_3]^{2-} + Cl_4catH_2 \quad (6)$$

isotropically shifted NMR spectra; resonances of m′ and m″ ligands are always well-resolved.[17,24,39] Coucouvanis and coworkers[23,40] have demonstrated a number of reactions in which bound catecholate can be substituted by the conjugate base chelate anion of di- or triprotic acids in proton transfer reactions. Cluster **6** has been prepared in this way;[23] in our hands, DMF rather than acetonitrile is the preferable solvent, affording higher yields and a cleaner product. Note that clusters **6**−**10,** as **4** and **5**, possess mirror symmetry and m′ and m″ iron sites, as shown for **6** in Figure 8. Cluster **6**, for example, shows H_a and H_b resonances at 14.9 and 5.85 ppm, respectively, in Me_2SO, as seen in Figure 9A. Clusters **8**−**10** were obtained in high yield by the standard ligand substitution reaction 7 (Figure 8). For **9** in particular, mirror symmetry is emphasized by the 44 ppm difference of the isotropically shifted SCH_2 protons at the m′ and m″ positions.

(39) (a) Mascharak, P. K.; Armstrong, W. H.; Mizobe, Y.; Holm, R. H. *J. Am. Chem. Soc.* **1983**, *105*, 475. (b) Zhang, Y.-P.; Bashkin, J. K.; Holm, R. H. *Inorg. Chem.* **1987**, *26*, 694.

(40) (a) Coucouvanis, D.; Demadis, K. D.; Kim, C. G.; Dunham, R. W.; Kampf, J. W. *J. Am. Chem. Soc.* **1993**, *115*, 3344. (b) Demadis, K. D.; Coucouvanis, D. *Inorg. Chem.* **1994**, *33*, 4195. (c) Demadis, K. D.; Malinak, S. M.; Coucouvanis, D. *Inorg. Chem.* **1996**, *35*, 4038.

Table 4. Selected Interatomic Distances (Å) and Angles (deg) for $[(Meida)VFe_3S_4Cl_3]^{3-}$ and $[(Meida)VFe_3S_4(O\text{-}p\text{-}C_6H_4Me)_3]^{3-}$

$[(Meida)VFe_3S_4Cl_3]^{3-}$		$[(Meida)VFe_3S_4(O\text{-}p\text{-}C_6H_4Me)_3]^{3-}$	
V(1)−O(3)	2.070(12)	V(1)−O(3)	2.065(10)
V(1)−O(4)	2.080(11)	V(1)−O(4)	2.095(9)
V(1)−N(1)	2.271(7)	V(1)−N(1)	2.297(11)
V(1)−S(2)	2.368(6)	V(1)−S(2)	2.326(4)
V(1)−S(3)	2.337(6)	V(1)−S(3)	2.357(4)
V(1)−S(4)	2.343(3)	V(1)−S(4)	2.366(4)
mean of 3	2.35(1)	mean of 3	2.35(2)
V(1)−Fe(1)	2.779(3)	V(1)−Fe(1)	2.799(3)
V(1)−Fe(2)	2.807(2)	V(1)−Fe(2)	2.785(3)
V(1)−Fe(3)	2.801(4)	V(1)−Fe(3)	2.804(3)
mean of 3	2.795(12)	mean of 3	2.796(8)
O(3)−V(1)−N(1)	77.6(5)	O(3)−V(1)−N(1)	77.2(4)
O(4)−V(1)−N(1)	75.8(5)	O(4)−V(1)−N(1)	77.3(4)
O(3)−V(1)−S(3)	89.3(4)	O(3)−V(1)−S(3)	88.7(3)
O(4)−V(1)−S(4)	89.0(4)	O(4)−V(1)−S(4)	86.5(3)
S(2)−V(1)−S(3)	100.4(1)	S(2)−V(1)−S(3)	102.1(2)
S(2)−V(1)−S(4)	103.0(2)	S(2)−V(1)−S(4)	102.5(2)
Fe−Fe range	2.690(3)−2.752(2)	Fe−Fe range	2.706(3)−2.754(3)
mean of 3	2.72(3)	mean of 3	2.74(2)
Fe−S range	2.259(6)−2.318(3)	Fe−S range	2.267(4)−2.328(5)
mean of 9	2.29(2)	mean of 9	2.29(2)
Fe(1)−Cl(3)	2.228(7)	Fe(1)−O(6)	1.872(10)
Fe(2)−Cl(1)	2.288(5)	Fe(2)−O(5)	1.894(9)
Fe(3)−Cl(2)	2.258(3)	Fe(3)−O(7)	1.897(10)
mean of 3	2.26(2)	mean of 3	1.89(1)

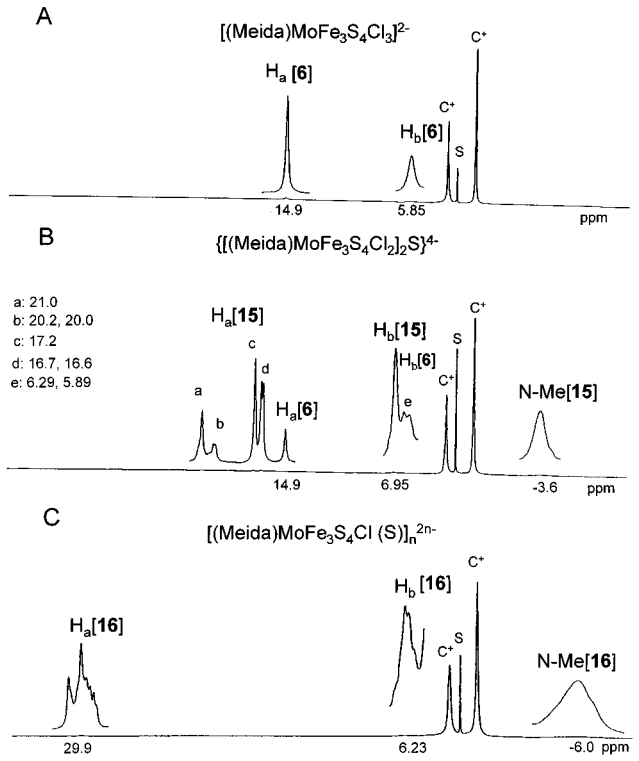

Figure 9. ^1H NMR spectra of the indicated clusters in Me_2SO solutions at ambient temperature (C^+ = cation, S = solvent). In spectrum B, signals a−e are associated with $\{[(Meida)MoFe_3S_4Cl_2]_2S\}^{4-}$. Other signal assignments in spectra A−C are indicated.

Reaction 8, conducted stoichiometrically in acetonitrile, was utilized to prepare a symmetrical sulfide-bridged double cubane containing molybdenum. The reaction system was heterogeneous because of the insolubility of Li_2S, which was added as a solid. Over the course of the reaction, the product separated as a dark brown solid. Its analysis is consistent with the formulation $(Et_4N)_4$[**15**]·2LiCl. The compound is freely soluble in DMF and Me_2SO, but is very sparingly soluble in acetonitrile. Because of this property, we were unable to separate the cluster product salt from LiCl. However, $(Et_4N)_2$[**6**], the precursor cluster salt, is freely soluble in acetonitrile. Any significant amount of this compound remaining from reaction 6 was removed by washing the reaction product with acetonitrile. The ^1H NMR spectrum in Me_2SO is complex, showing six separate signals (H_a) at 16−21 ppm, at least two signals at 6−7 ppm (H_b), and also the H_a,H_b signals of single cubane **6** (Figure 9B). The identity of the reaction product is demonstrated by two lines of evidence. As shown in Figure 10, the observed pattern in the negative-ion ESMS centered at about *m*/*z* 754 corresponds to the ion $[\mathbf{15}\cdot 2Et_4N^+]^{2-}$. The cyclic voltammogram of the reaction product in Me_2SO, available in Figure 6 (lower), exhibits two well-defined reductions at −1.01 and −1.34 V. Consistent with the behavior of bridged double cubanes **11**−**13**, the first step is shifted strongly negative of the precursor single cubane **6** (by 170 mV, Table 3) and the two reductions are well-resolved with the potential separation (330 mV) close to the preceding range. These results identify the reaction product as sulfide-bridged double cubane **15** (Figure 8), the desired product. Despite numerous attempts, we have thus far not been able to achieve diffraction-quality crystals of any material containing **15**. Because of this situation, involving **15** and other double cubanes (not reported here), the ESMS and voltammetric criteria for sulfide/selenide-bridged double cubanes were developed.

$$2[(Meida)MoFe_3S_4Cl_3]^{2-} + Li_2S \rightarrow \{[(Meida)MoFe_3S_4Cl_2]_2S\}^{4-} + 2LiCl \quad (8)$$

We have also examined the origin of single cubane **6** in solutions of **15**. The ^1H NMR spectra of a Me_2SO solution prepared from $(Et_4N)_4$[**15**]·2LiCl at 307−377 K in the H_a region are presented in Figure 11. The signal assigned to **6** is at exactly the same position as in a solution prepared from $(Et_4N)_2$[**6**] separately. At 307 K, the mole ratio [**15**]/[**6**] ≈ 3.2:1. As the temperature is increased, this ratio decreased, and at 377 K, [**15**]/[**6**] ≈ 0.6:1. Given the minor amount or absence of $(Et_4N)_2$-[**6**] in the isolated product of reaction 8, we conclude that double cubane **15** is cleaved to **6** by chloride; i.e., the reverse of reaction 8. In Me_2SO solution, where all components are soluble, this reaction is an equilibrium process. Addition of sufficient chloride reduces or eliminates the resonances of **15**. These

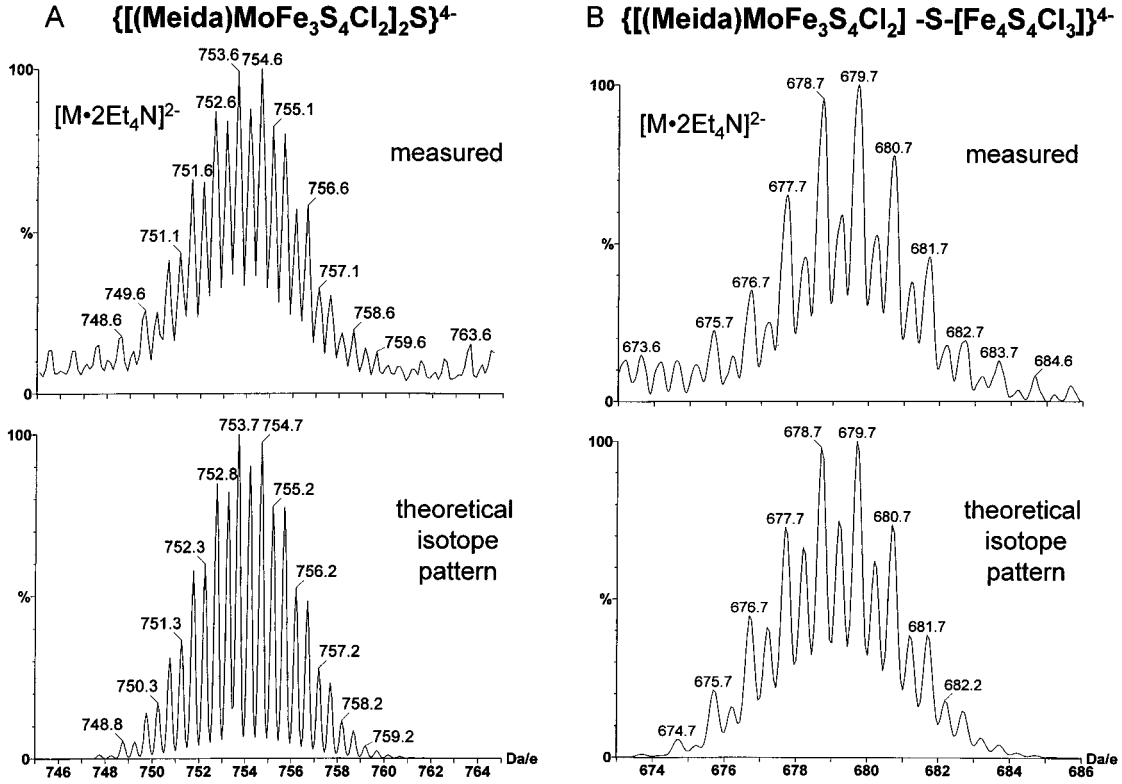

Figure 10. Measured negative-ion ESMS of $\{[(Meida)MoFe_3S_4Cl_2]_2S\cdot 2Et_4N^+\}^{2-}$ (A) and $\{[(Meida)MoFe_3S_4Cl_2]S(Fe_4S_4Cl_3)\cdot 2Et_4N^+\}^{2-}$ (B). Measured spectra are at the top and theoretical isotope patterns below. The compound $(Et_4N)_4\{[(Meida)MoFe_3S_4Cl_2]_2S\}\cdot 2LiCl$ and the isolated product from reaction 11 were sampled from DMF solutions.

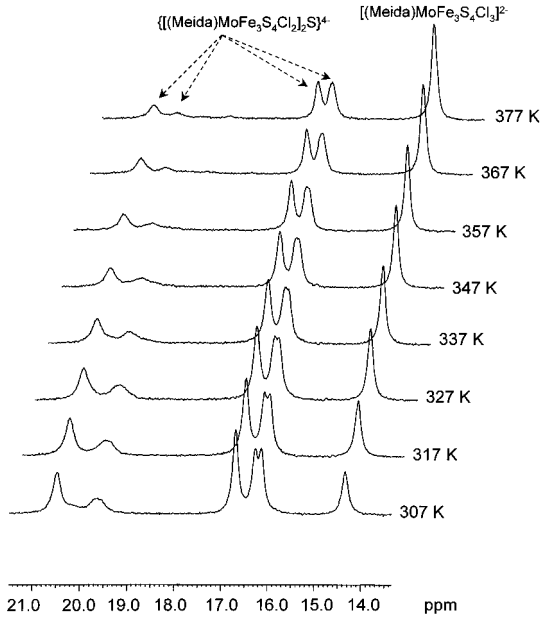

Figure 11. ^{1}H NMR spectra at 307−377 K of a Me_2SO solution prepared from $(Et_4N)_4\{[(Meida)MoFe_3S_4Cl_2]_2S\}\cdot 2LiCl$, proving the coexistence of **15** and **6**, with the proportion of the latter increasing with increasing temperature. The spectra are in the H_a region (cf. Figure 9).

observations provide the informative result that pure solutions of sulfide-bridged double cubanes cannot accommodate certain exogenous species (e.g., chloride, thiolate, phenolate) that are competitive ligands at the bridge iron sites.

(ii) Isomers. The multiple H_a,H_b NMR signals evident in Figure 9B are rationalized upon further consideration of the structure of **15**. This double cubane cluster can exist as a mixture of *four* geometrical isomers, which are specified in Figure 12. Three isomers arise because the individual cubanes can be bridged through m′/m′ (C_{2v}), m″/m″ (C_2, C_s), and m′/m″ (C_1) sites. (The point groups refer to the most symmetric cluster conformations.) The m″/m″ bridging mode develops two isomers because in the indicated conformations the two Meida chelate units can be related by either a 2-fold axis or a mirror plane (equivalently, the Meida nitrogen atoms can be transoid or cisoid around the Fe−S−Fe bridge). This situation generates a total of nine H_a and nine H_b resonances. As previously noted, six H_a features are resolved in the spectrum at ambient temperature.

To provide further confirmation of the presence of isomers of **15**, we prepared single cubane **10** by reaction 7 (Figure 8) and thereafter generated in situ in Me_2SO the double cubane product of reaction 9. These experiments were predicated on

$$\{[(Meida)MoFe_3S_4Cl_2]_2S\}^{4-} + 4p\text{-}FC_6H_4S^- \rightarrow \{[(Meida)MoFe_3S_4(SC_6H_4\text{-}p\text{-}F)_2]_2S\}^{4-} + 4Cl^- \quad (9)$$

the extreme sensitivity of isotropically shifted ^{19}F resonances to cluster structure.[17,41] The m′ (−80.8 ppm) and m″ (−99.4 ppm) signals of **10** are separated by 18.6 ppm and appear in the spectrum of reaction 9 (not shown) as a secondary product. Also present are some eight additional signals,[42] not all of equal intensity; these are sensibly assigned to the double cubane reaction product, a full isomeric mixture of which would generate nine signals. Because we used 5 equiv of thiolate in the reaction, it is unlikely that any of these signals arise from

(41) Mascharak, P. K.; Smith, M. C.; Armstrong, W. H.; Burgess, B. K.; Holm, R. H. *Proc. Natl. Acad. Sci. U.S.A.* **1982**, *79*, 7056.

(42) ^{19}F resonances assigned to the double cubane reaction product: −73.1 (C_1), −77.7, −77.8, −80.3, −80.5 (C_1), −83.1, −83.9 (C_1), −84.8 (C_1) ppm. Those assigned to the C_1 isomer are indicated. Of these signals, all but that at −80.5 ppm were fully resolved and shown to have a 1:1:1 intensity ratio.

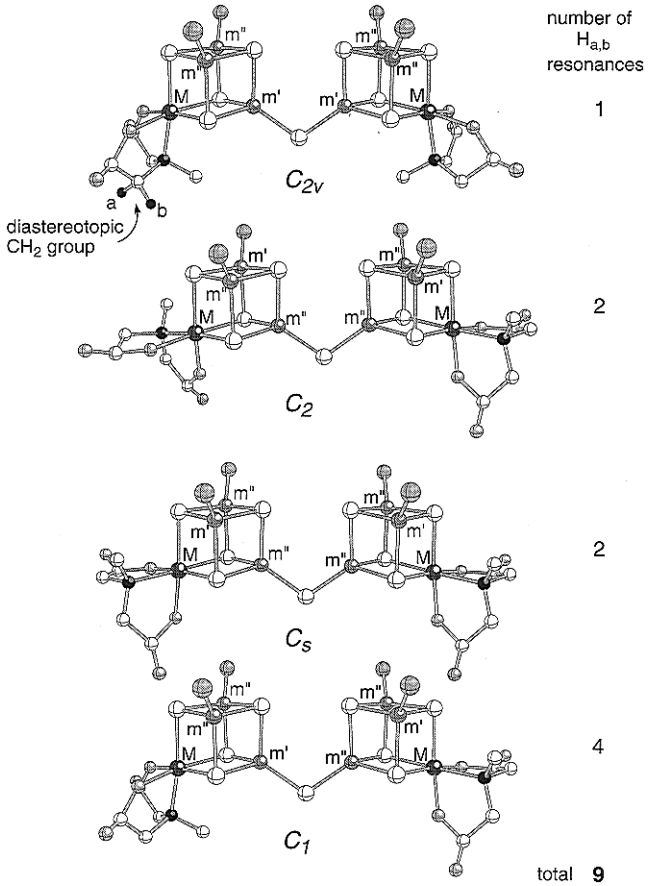

Figure 12. Geometrical isomers of sulfide-bridged double cubanes in which the M site is not trigonally symmetric. In these examples, the Meida ligand is used. Note that each ligand has two diastereotopic methylene groups with protons H_a and H_b. The number of ^1H NMR resonances refers to either H_a or H_b.

incompletely substituted clusters. Excess thiolate contributes to the formation of **10**. Upon standing for 2 days at ambient temperature, the reaction mixture retained the same eight signals but the relative intensities of some changed. From this observation, it was possible to assign four signals to the C_1 isomer[42] (Figure 12), which has no symmetry and, therefore, one m′ site and three different m″ sites. Inspection of the conformations of the four isomers (vide infra) indicates that C_1 isomer does not possess as sterically crowded conformations as do the other three and should be the most stable. The collective ^1H and ^{19}F NMR results are fully consistent with isomeric sulfide-bridged double cubanes; the existence of isomers contributes to the structure proof.

The existence of an isomeric mixture presumably contributes to our inability to obtain single crystals of a salt of **15**. The NMR complexity and, perhaps, the difficulty in obtaining single crystals of a double cubane compound would be removed by the introduction of a 3-fold symmetric ligand at the molybdenum site. However, given the currently available synthetic routes to $MoFe_3S_4$ single cubanes,[17,24,39] the synthesis of a Mo site-protected cluster of trigonal symmetry is not an elementary matter. For now, we choose to investigate the more readily available clusters.

(iii) Multiply Bridged Cluster. Double cubane **15** reacts further with Li_2S. Treatment of the cluster in Me_2SO with slightly more than 1 equiv of solid Li_2S abolishes all signals of **15**, causing the appearance of a new set of signals. At least eight H_a and four H_b signals are discernible together with a broad N-Me feature at −6.0 ppm (Figure 9C); no other resonances were detected. We formulate the product of reaction 10a as a multiply bridged cluster **16,** which is expected to have four (n = 2) or numerous (n > 2) geometrical isomers. This cluster can also be prepared directly by reaction of **6** with 1 equiv of solid Li_2S in Me_2SO in reaction 10b and isolated as a dark brown

$$(n/2)\{[(\text{Meida})MoFe_3S_4Cl_2]_2S\}^{4-} + (n/2)Li_2S \rightarrow \{[(\text{Meida})MoFe_3S_4Cl]S\}_n^{2n-} + n\text{LiCl} \quad (10a)$$

$$n[(\text{Meida})MoFe_3S_4Cl_3]^{2-} + nLi_2S \rightarrow \{[(\text{Meida})MoFe_3S_4Cl]S\}_n^{2n-} + n\text{LiCl} \quad (10b)$$

solid in 67% yield. The IR spectrum of **16** is very similar to that of **15**; in the carboxylate region, a single strong but broadened ν_{COO} band is observed at 1636 cm^{-1}. It is important to observe that, when Li_2S is less than 1 equiv in reaction system 10a, no change occurs in the intensity ratio of NMR peaks a−d (Figure 9B). This observation supports the assignment of these signals to the four isomers of **15** rather than of clusters with different numbers of sulfide bridges.

At the current stage, we do not know the structure of **16**. However, its multiple sulfide-bridged polycubane nature is consistent with the following observations. (i) Reaction of **16** with n equiv of **6** in Me_2SO immediately produces an NMR spectrum identical with Figure 9B, indicating the formation of **15** as the *sole* detectable product. Evidently, **16** sacrificially functions as a sulfide source, converting single cubane **6** partially to **15**. (ii) In Me_2SO at elevated temperatures, **16** is unstable and passes to a mixture of **6** and **15**. (iii) Two irreversible reductions are observed in cyclic voltammetry at $E_{pc} = -1.49$ and −1.72 V in DMF. The first reduction occurs at a potential estimated at about 80 mV more negative than the second reduction of **15**. In keeping with trends in potentials (Table 3), this indicates a cluster negative charge exceeding 4−. We regard **16** with $n = 4$, a cyclic tetracubane with no evident ring strain, as a likely formulation. The $n = 2$ structure requires the roughly parallel orientation of cubane faces across two Fe−S−Fe bridges, bringing these faces into an arrangement disfavored by intercubane repulsive interactions.

(c) Formation of an Unsymmetrical Sulfide-Bridged $MoFe_3S_4/Fe_4S_4$ Double Cubane. Although a number of symmetrical bis-$MoFe_3S_4$ double cubanes have been prepared,[15] only one cluster containing two different bridged cubanes has been claimed. The species $[(Cl_4cat)MoFe_3S_4Cl_2(\mu_2\text{-}S)_2Fe_4S_4\text{-}Cl_2]^{5-}$ obtained by a sulfide coupling reaction in acetonitrile, is described as containing Mo−S−Fe and Fe−S−Fe bridges between individual cubane clusters.[43] This formulation is based solely on elemental analysis of a Et_4N^+ salt; the atom ratio Mo:Fe:S = 1:6.5:9.1 approaches the desired $MoFe_7S_{10}$ core composition. The analysis cannot distinguish pure clusters and certain mixtures of clusters; the solution behavior of the cluster product has not been described. Any ultimately successful prosecution of the scheme in Figure 1 requires an unsymmetrical cluster **2** with M = Mo and Fe. Consequently, we have investigated the matter of unsymmetrical double cubane formation in solution.

Reactions 11 and 12 in Me_2SO solutions were examined. For reaction 11, an equimolar ratio of reactants afforded a homogeneous dark brown solution. Addition of THF/ether (1:1 v/v) to the solution caused the separation of a dark brown solid which was shown to contain the unsymmetrical double cubane **17** (Figure 8) and the symmetrical coupling product **15**. We have demonstrated that both reactions are reversible equilibria. The

(43) (a) Coucouvanis, D.; Challen, P. R.; Koo, S.-M.; Davis, W. M.; Butler, W.; Dunham, W. R. *Inorg. Chem.* **1989**, *28*, 4183. (b) Coucouvanis, D. *Acc. Chem. Res* **1991**, *24*, 1.

$$3[(\text{Meida})MoFe_3S_4Cl_3]^{2-} + 3[Fe_4S_4Cl_4]^{2-} + 3Li_2S \rightleftarrows \{[(\text{Meida})MoFe_3S_4Cl_2]S(Fe_4S_4Cl_3)\}^{4-} + \{[(\text{Meida})MoFe_3S_4Cl_2]_2S\}^{4-} + [(Fe_4S_4Cl_3)_2S]^{4-} + 6LiCl \quad (11)$$

$$\{[(\text{Meida})MoFe_3S_4Cl_2]_2S\}^{4-} + [Fe_4S_4Cl_4]^{2-} \rightleftarrows \{[(\text{Meida})MoFe_3S_4Cl_2]S(Fe_4S_4Cl_3)\}^{4-} + [(\text{Meida})MoFe_3S_4Cl_3]^{2-} \quad (12)$$

^{1}H NMR spectrum of the isolated solid from reaction 11 is presented in Figure 13A. In addition to a minor quantity of **6** and a larger amount of **15**, new species are present that afford H_a signals at 22.0 and 28.8 ppm, an H_b signal at 8.60 ppm, and N-Me resonances at −5.8 and −8.4 ppm (compare with Figure 9A,B). The appearance of two H_a *and* two N-Me signals, both in an intensity ratio of ca. 4:1, is entirely consistent with the formation of **17**, which can exist as two isomers (Figure 13) depending on whether the bridge is made at an m′ or m″ site. The mole ratio **17**:**15**:**6** ≈ 9:3:1 at the concentration specified in Figure 13A. When the solid is treated with acetonitrile, the solution contains only **17** as detected by NMR, owing to the low solubility of $(Et_4N)_4$[**15**]. Reaction 11 is written with the simplest stoichiometry, showing equimolar amounts of cluster products, but this need not be the case. The clusters $[Fe_4S_4Cl_4]^{2-}$ and **11** are not detectable by NMR. When reaction 12 is conducted with equimolar reactants and examined in situ, the spectrum of Figure 13B is observed. Double cubane **17** is again formed together with a larger amount of **6** than in reaction 11, inasmuch as it is a product and not a reactant. Residual reactant **15** was also detected.

In addition to the foregoing NMR evidence, the formulation of **17** as an unsymmetrical sulfide-bridged double cubane is supported by other evidence. (i) The negative-ion ESMS of the product of reaction 11 develops a prominent pattern centered near *m*/*z* 679 whose isotope pattern matches very well that calculated for [**17**·2Et_4N^+]. Experimental and theoretical spectra in this region are compared in Figure 10. The spectrum also contains small amounts of $[Fe_4S_4Cl_4]^{2-}$ and **6** and a trace of **15**. ESMS spectra, however, do not necessarily reflect equilibrium solution compositions.[32b,44] (ii) The cyclic voltammogram of the material in i shows three well-defined peaks at $E_{1/2}$ = −0.82, −1.03, and −1.27 V in DMF solution. The first feature corresponds to the reduction of **6**, while the other two are consistent with the reduction of a mixture of **15** and **17**. Given the potentials of the single cubanes $[Fe_4S_4Cl_4]^{2-}$ and **6**, the potentials of double cubanes **15** and **17** are unlikely to be resolvably different.

(d) Relative Stabilities of Sulfide-Bridged Double Cubanes. From ^{57}Fe isomer shifts, we have proposed the oxidation state description $Mo^{3+}Fe_3^{2.67+}$ for $[MoFe_3S_4]^{3+}$ clusters.[34c,45] The clusters $[Fe_4S_4L_4]^{2-}$ contain $Fe^{2.5+}$. On this basis, sequence 13

$$[MoFe_3S_4]^{3+}-S-[MoFe_3S_4]^{3+} > [MoFe_3S_4]^{3+}-S-[Fe_4S_4]^{2+} > [Fe_4S_4]^{2+}-S-[Fe_4S_4]^{2+} \quad (13)$$

is a reasonable stability order for Fe−S−Fe bridges. On the other hand, **15** and **17** are potentially destabilized by conformations which bring the rigid Meida chelate ring moiety into proximity with another such moiety (**15**) or with a chloride atom

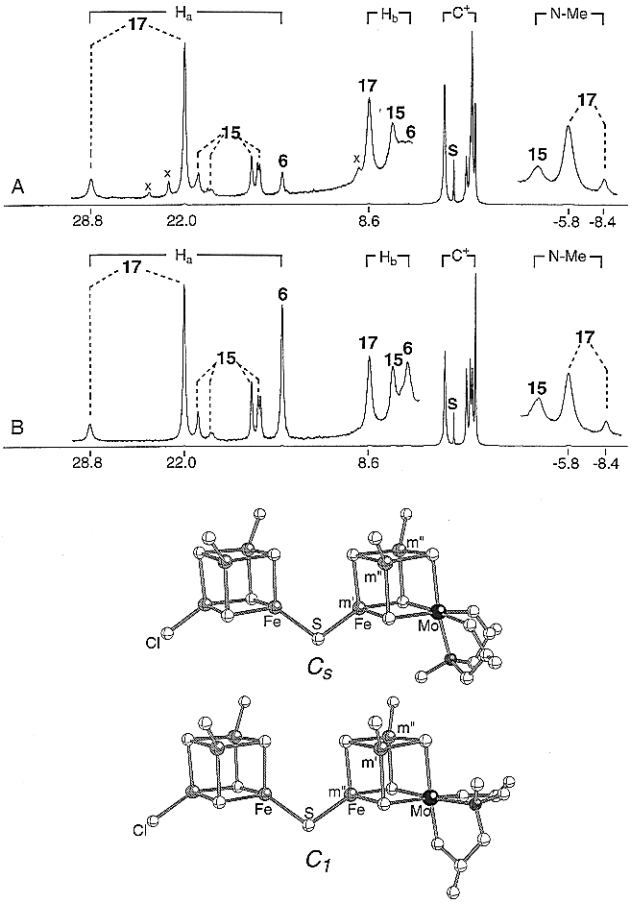

Figure 13. ^{1}H NMR spectra in Me_2SO: (A) the solid product (40 mg/mL) isolated from reaction 11; (B) *in situ* products of reaction 12. Spectrum A was recorded with 20 mg of the reaction product in 0.5 mL of Me_2SO. At lower concentrations, the impurity signals (x) are absent. C^+ = Et_4N^+ and Bu_4N^+, and S = solvent. The two isomers of $\{[(\text{Meida})MoFe_3S_4Cl_2]S(Fe_4S_4Cl_3)\}^{4-}$ are depicted.

(**17**) across the bridge. We have examined this matter by computer modeling. Because the structures of the double cubanes are not available, we have employed the structural parameters of **6**[23] and $[Fe_4S_4Cl_4]^{2-}$,[46] and taken the Fe−S bridge bond lengths in the fragments Fe_4S_4−S and $MoFe_3S_4$-S as 2.21 and 2.19 Å, respectively, as reported for **11**[20] and $\{[(C_2O_4)\text{-}MoFe_3S_4]_2(\mu_2\text{-CN})(\mu_2\text{-S})\}^{5-}$.[23] We define the "least-crowded" Fe−S−Fe bridge angle as that which corresponds to the smallest intercubane angle consistent with free rotation of the individual cubanes about the bridge Fe−S bonds. This angle is determined by setting the distance between the closest nonbonding atoms in the most crowded conformation as the sum of their van der Waals radii.

The most useful conclusions from the steric analysis are summarized in Figure 14. Of the four isomers of **15**, the C_1 isomer has the smallest noncrowded angle in the most congested conformation and thus is the most stable isomer. Both isomers of **17** have less crowded angles than **15**, and that for the C_1 isomer is the lesser of the two. Under the proposition that the increasing deviation from the essentially unstrained bridge angle of 102° in **11** is the direction of steric obstruction, the stability sequence 14 follows.

$$\textbf{17}\ (C_1) > \textbf{17}\ (C_s) > \textbf{15}\ (C_1) > \textbf{15}\ (C_{2v}, C_2, C_s) \quad (14)$$

The mole ratio **17**:**15** ≈ 3:1 for the products of reaction 11 is consistent

(44) Leize, E.; Van Dorsselaer, A.; Krämer, R.; Lehn, J.-M. *J. Chem. Soc., Chem. Commun.* **1993**, 990.

(45) Mascharak, P. K.; Papaefthymiou, G. C; Armstrong, W. H.; Foner, S.; Frankel, R. B.; Holm, R. H. *Inorg. Chem.* **1983**, *22*, 2851.

(46) Bobrik, M. A.; Hodgson, K. O.; Holm, R. H. *Inorg. Chem.* **1977**, *16*, 1851.

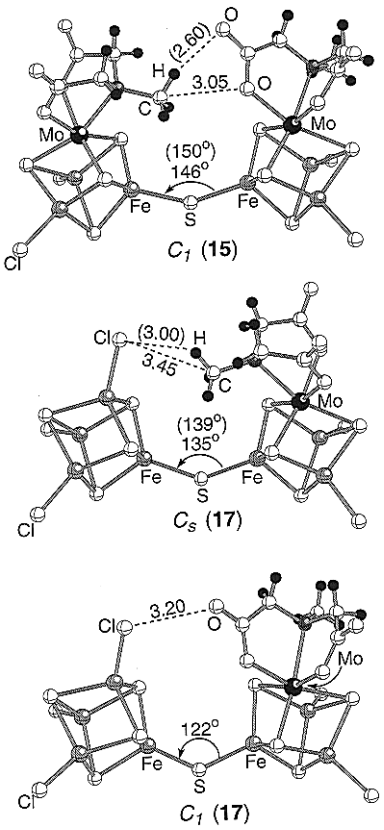

Figure 14. Depictions of the most crowded conformations of the C_1 isomer of symmetrical double cubane **15** and the two isomers of unsymmetrical double cubane **17**. Distances (Å) corresponding to van der Waals contacts are indicated. Bridge angles with and without parentheses correspond to the inclusion or noninclusion, respectively, of a hydrogen atom in the pair of closest atoms across the bridge. The difference in angle is unimportant to the argument. The van der Waals radii (Å) used: C, 1.65; O, 1.40; Cl, 1.80; H, 1.20.

with this order and not with sequence 13. On this basis, we associate the intense signal at 22.0 ppm in the NMR spectrum of **17** (Figure 13) with the C_1 isomer. Indeed, manipulation of steric factors may allow a much higher product ratio in favor of the unsymmetrical double cubane, but with the unavoidable formation of symmetrical **11**.

Summary. The following are the principal results and conclusions of this investigation.

(1) The symmetrical double cubanes with the core structure $[Fe_4S_4-S-Fe_4S_4]^{2+}$ (**11**, **12**) were obtained by the reaction of $[Fe_4S_4Cl_4]^{2-}$ and of the [1:3] site-differentiated single cubane $[Fe_4S_4(LS_3)Cl]^{2-}$ with solid Li_2S. The double cubane $[Fe_4Se_4-Se-Fe_4Se_4]^{2+}$ (**13**) was obtained by an analogous reaction of $[Fe_4Se_4(LS_3)Cl]^{2-}$ and Li_2Se. Similarly, the trigonal cuboidal cluster $[VFe_4S_6(PEt_3)_4Cl]$ has been coupled to form **14**. The bridged double cubane structures of **11**[20] and **13** and the bridged structure of **14** have been proven crystallographically.

(2) For the clusters in 1, additional criteria for the Fe−S−Fe double cubane structure were developed using cyclic voltammetry, which revealed coupled reductions (**11**−**14**) and oxidations (**14**) and electrospray mass spectrometry, which detected intact clusters (**11**, **14**). With the double cubanes, successive reduction steps are separated by 240−310 mV (**11**−**13**).

(3) The $[VFe_3S_4]^{2+}$ single cubanes **4** and **5** were prepared. Together with the $[MoFe_3S_4]^{3+}$ single cubane **6**,[23] their structures define the tight tricoordinate (Meida)M structural fragment imposed to confine the bridge-forming reactions in 4 and 5 to iron sites.

(4) Given the results in 1 and the structural feature in 3, single cubane **6** was coupled using Li_2S to afford the symmetrical double cubane **15**, which was isolated. The double cubane structure was established by the criteria in 2. Also, the existence of four isomers (^{1}H NMR) augments the structure proof. Isomers arise because of the mirror symmetry of individual clusters; the absence of isomers requires trigonal symmetry at the heterometal site. In the presence of excess chloride, **15** is partially cleaved to **6** in an equilibrium reaction.

(5) The equimolar reaction system **6**:$[Fe_4S_4Cl_4]^{2-}$:Li_2S afforded **15**, **17**, and, presumably, **11**. Cluster **17** was also produced in the system **15**:$[Fe_4S_4Cl_4]^{2-}$. The sulfide-bridged double cubane structure of **17** is supported by the criteria in 2 and by the existence of two isomers (^{1}H NMR).

(6) The core composition of double cubane **15** ($Mo_2Fe_6S_9$) approaches that of FeMoco ($MoFe_7S_9$). The core composition of **17** is exactly the same as FeMoco; **17** is the first synthetic cluster with this property.

This research provides the first comprehensive study of the synthesis, structures, and properties of a new class of clusters, the sulfide-bridged double cubanes. In future reports, we will further develop this cluster class and describe the efficacy of core rearrangement reactions, such as **2** → **3** (Figure 1).

Acknowledgment. This research was supported by NIH Grant GM 28856. X-ray diffraction equipment was obtained by NIH Grant 1 S10 RR 02247. The mass spectrometry facility at Harvard University is funded by NIH Grants S10 RR 06716 and S10 RR 08458 and by NSF Grant CHE 90-20043. We are indebted to Drs. R. J. Staples and A. Tyler for invaluable assistance with crystallography and mass spectrometry, respectively. During this research, H.A. was on leave from the Department of Chemistry, Okayama University of Science.

Supporting Information Available: X-ray structural information for the compounds in Table 1, including tables of crystal and intensity collection data, positional and thermal parameters, and interatomic distances and angles (75 pages). See any current masthead page for ordering and Internet access information.

JA971401Q